INVITED PAPER

Silicon Nanocrystals as an Enabling Material for Silicon Photonics

With better control and optimization and more knowledge about these crystals, they may become increasingly useful for improving fast all-optical switches.

By Zhizhong Yuan, Aleksei Anopchenko, Nicola Daldosso, Romain Guider, Daniel Navarro-Urrios, Alessandro Pitanti, Rita Spano, and Lorenzo Pavesi

ABSTRACT | Silicon nanocrystals (Si-nc) is an enabling material for silicon photonics, which is no longer an emerging field of research but an available technology with the first commercial products available on the market. In this paper, properties and applications of Si-nc in silicon photonics are reviewed. After a brief history of silicon photonics, the limitations of silicon as a light emitter are discussed and the strategies to overcome them are briefly treated, with particular attention to the recent achievements. Emphasis is given to the visible optical gain properties of Si-nc and to its sensitization effect on Er ions to achieve infrared light amplification. The state of the art of Si-nc applied in a few photonic components is reviewed and discussed. The possibility to exploit Si-nc for solar cells is also presented. In addition, nonlinear optical effects, which enable fast all-optical switches, are described.

KEYWORDS | Amplification; nanosilicon; nonlinear properties; photonics

I. INTRODUCTION

Photonics is becoming increasingly important in electronics since it can keep pace with both the "more-Moore" (higher performances by increasing integration and parallelism) and "beyond-Moore" (new computation principles) evolution trends of electronics. Silicon photonics, pioneered by Soref in the 1980s [1], [2], is a technology that can merge both electronics and photonics in a single chip to take advantage of both technologies: the high computation capability of electronics and the high communication bandwidth of photonics. The main interest of silicon photonics is associated with the possibility of adding new functionalities to electronic components such as low propagation losses, high bandwidth, wavelength multiplexing, and immunity to electromagnetic noise. The main strength of this technology is that the silicon properties of low cost, nontoxicity, and sophisticated ultra-large-scale integrated (ULSI) circuit fabrication technology, that were responsible of the great success of silicon in electronics, can be put to the best use. Silicon photonics is not only a promising research field but also a reality with the presence of the first commercial devices that can be applied to a wide range of application fields [3].

Since silicon is a good optical material but is a poor light emitter, the discovery of light emission from porous silicon at room temperature in 1990 [4] boosted the research on all silicon-based light sources. At the same time, the concept of silicon microphotonics or optoelectronics emerged impetuously [5]–[7]. At the end of the last century, the heterogrowth of germanium on silicon was mastered, allowing the development of high-speed complementary metal–oxide–semiconductor (CMOS) compatible optical receivers [8], [9]. At the same time, silicon-based waveguides were shrinking in size: from more than 100 μm^2 typical of waveguides based on refractive index contrast given by different doping levels during

Manuscript received December 1, 2008. Current version published June 12, 2009. This work was supported by the European Commission under the PHOLOGIC (FP6-017158), LANCER (FP6-033574), POLYCERNET (MCRTN-019601), WADIMOS (FP7-216405) and HELIOS (FP7-224312) projects, by PAT under the HCSC and NAOMI projects, and by Intel.
Z. Yuan, **A. Anopchenko**, **N. Daldosso**, **R. Guider**, **A. Pitanti**, **R. Spano**, and **L. Pavesi** are with the Nanoscience Laboratory, Department of Physics, University of Trento, 38100 Povo-Trento, Italy (e-mail: ryanyuan@science.unitn.it; anopchenko@science.unitn.it; daldosso@science.unitn.it; guider@science.unitn.it; pitanti@science.unitn.it; spano@science.unitn.it; pavesi@science.unitn.it).
D. Navarro-Urrios is with the Departament d'Electrònica, Universitat de Barcelona, 08028 Barcelona, Spain (e-mail: dnavarro@el.nb.es).

Digital Object Identifier: 10.1109/JPROC.2009.2015060

 0018-9219/$25.00 ©2009 IEEE

the 1980s to 5 μm^2 size of rib waveguides, where Si/SiO_2 was used to give index contrast.

Since 2000, silicon photonics has boomed and tremendous efforts have been invested in this field. Many important breakthroughs have been obtained on light emitters [10]–[15], waveguides [16]–[21], modulators [22], [23], microcavities and resonators [24]–[26], and detectors [27], [28].

Silicon photonics is also attracting the attention of industry. Many companies are eager to perform research and get actual commercial opportunities [29], [30]. In 2002, ST-microelectronics [31] in Italy reported highly efficient electroluminescence (EL) from an Er-doped device. In 2003, photonic bandgap waveguides with low losses were demonstrated by IBM [32]. In 2004, low-loss silicon wire waveguides and a 30 GHz SiGe photodetector were fabricated at IBM [33], [34]. A modulator with modulation bandwidth exceeding 1 GHz was fabricated at Intel [35]. Moreover, wavelength conversion [36] and all-optical switching in silicon were proposed [37], [38]. In 2005, a continuous wavelength (CW) silicon Raman laser was introduced by Intel [39], and a 10 Gbps modulator was demonstrated independently both by Intel [40] and Luxtera [41]. In 2006, a hybrid silicon evanescent laser was invented by the University of California Santa Barbara and Intel [42], and a broadband amplifier based on Raman gain was introduced by Cornell [43]. Furthermore, the electrooptical effect in strained silicon was demonstrated [44]. Up to 16 cascade ring add/drop filters were produced by IBM [45]. A microdisk laser was coupled to silicon waveguides by IMEC and LETI [46]. In 2007, the device performances reached 40 Gbps for active silicon photonics devices at Intel: a mode-locked silicon evanescent laser [47], a fast Ge photo-detector [48], and a modulator [49]. Luxtera launched its first photoreceiver: a four-channel 10 Gbps monolithic optical receiver in 130 nm CMOS with integrated Ge waveguide photodetectors [50]. The IBM team demonstrated optical buffering of 10 bits at 20 Gbps in 100 cascaded ring resonators [51] and, recently, fast optical switching [52]. In 2008, Lightwire launched high-speed interconnects project based on its patented silicon photonics-based optical application specific integrated circuit interconnect platform. Kotura realized the first example of a successful silicon photonics-based product: the UltraVOA array, which provides simple current-controlled optical attenuation (0–40 dB) and enables ultrafast (300 ns) power management in optical networks.

We can see that silicon photonics is really booming. It involves the invention of new structures and, more importantly, the application of new materials or of new phenomena in existing materials. Silicon nanocrystal (Si-nc, Si-ncs) embedded in a dielectric matrix (in most cases, silicon oxide) is one of the important materials, which has already made great contributions to these breakthroughs mentioned above and will continue to improve the performance of various kinds of devices. Therefore, the fundamental physics and applications of Si-nc as an enabling material for silicon photonics are reviewed in this paper. First, we will look at the main obstacles for bulk silicon to be an efficient light emitter and list some important approaches to enhance the light emission from silicon. Then, we address Si-nc as light emitters and, more importantly, the main achievements so far to get optical gain from this system. In the sixth section, we will give a brief introduction on applications of Si-nc other than light emitters, such as waveguides, resonant cavities and solar cells, etc., and we will also address the nonlinear effect of Si-nc. Lastly, we will draw conclusions and point out future perspectives.

II. WHY CAN SILICON NOT BE USED AS A LASER MATERIAL?

The most difficult optical device to be made from silicon is a light emitter. Let us try to understand why silicon is not a good light emitting material [53].

Fig. 1 is a simplified energy band diagram of silicon. The main limitation to using silicon as a light source is related to its indirect bandgap structure, which implies low radiative recombination efficiency due to the need of the assistance of a phonon to fulfill momentum conservation. This in turn means that electron-hole (e-h) pairs have very long radiative lifetimes, in the millisecond range. This is

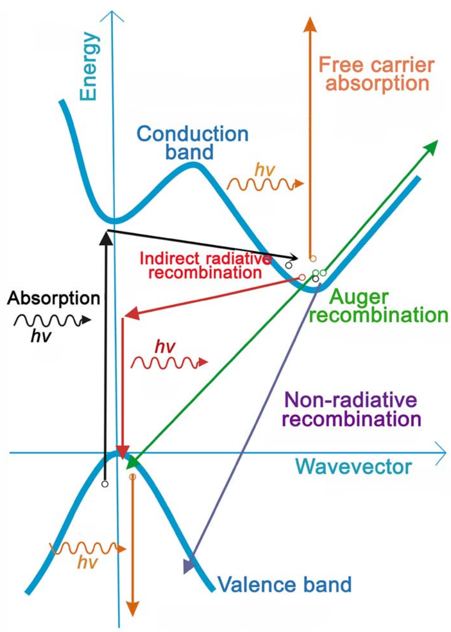

Fig. 1. *Schematic energy band diagram of silicon. The various arrows indicate the recombination paths for an excited electron and absorption processes. Black arrows: indirect absorption. Red arrows: indirect radiative recombination with the assistance of a phonon. Blue arrow: nonradiative recombination. Green arrows: Auger recombination. Orange arrows: free-carrier absorption.*

not a problem *per se* for light emission. The problem comes from the fact that e-h pairs in silicon move freely, on average a distance of a few micrometers, before recombining. Thus, the probability of encountering defects or luminescence killer centers is high, even in electronic grade silicon. Consequently, the nonradiative recombination lifetime in silicon is a few nanoseconds long, i.e., most of the excited e-h pairs recombine nonradiatively. This translates into very low internal quantum efficiency at room temperature, $\sim 10^{-6}$. Moreover, when population inversion is needed to achieve lasing, high excitation is needed. Under this condition, fast nonradiative processes turn on such as Auger recombination (participation of three particles in nonradiative processes, green arrows in Fig. 1) or free carrier absorption (orange arrows in Fig. 1). Both these processes deplete the excited population and provide loss mechanisms. Therefore, silicon is considered out of the list of light emitter candidates.

III. DIFFERENT APPROACHES TO OVERCOME SILICON'S LIMITATIONS

Taking into account these limitations, many strategies have been proposed to improve the light emission from silicon [3], [54], [55].

1) Porous silicon [4], [56], [57]: it can be fabricated electrochemically by dissolving silicon into HF solution.
2) Nanosized silicon or silicon p-n junctions: for the former, stimulated emission at 1.28 μm was obtained at cryogenic temperature [58]. For the latter, large quantities of carriers were confined and stimulated light emission was achieved [14].
3) Bulk silicon p-n junction: extremely pure bulk silicon was used to fabricate a p-n junction with solar cell characteristics to eliminate most of the nonradiative centers and get more photons out of the front surface of the device [59]. Another kind of efficient bulk silicon p-n junction light emitter is based on dislocation loops, which are resulted from ion implantation and annealing [60]–[63]. Carriers are confined at edges of dislocation loops and cannot diffuse to nonradiative centers, and thus the radiative recombination can be enhanced.
4) Brillouin zone folding and band structure engineering. It can be achieved by using group IV elements to alloy with Si or to fabricate nanostructures [3], such as SiGe quantum wells, Si/Ge superlattices, GeSi and SiC alloys, etc. Moreover, high gain and luminescence intensity in strained Ge on Si at room temperature was predicted [64].
5) Dislocation-related luminescence: the carriers recombine radiatively at specific type of dislocations [65], [66].
6) Incorporating a direct bandgap compound, for example, β-$FeSi_2$ [67], [68], into silicon.
7) Raman laser: an all-silicon Raman laser has been successfully fabricated [39], [69] by standard CMOS techniques.
8) III–V compound laser bound to silicon substrate [42].
9) Rare-earth ions as luminescence centers [18], [70]–[73].
10) Si-nc based light emitters, which will be introduced in detail in the next section.

IV. Si-nc BASED LIGHT EMITTERS

The realization of a silicon-based light emitter via Si-nc was motivated by the discovery of light emission from porous silicon. It has been greatly advanced by different kinds of fabrication techniques. Its study is actually focused on two directions: photoluminescence (PL), with the aim to distinguish the origin of the light emission where some issues are still controversial; and EL with injection-based devices, which still suffer from low efficiency.

There are various techniques to fabricate Si-nc, whose size can be tailored to a few nanometers. The choice among them depends on the particular application one is interested in. Bottom-up approaches rely on the direct chemical synthesis of Si-nc by chemical reactions of suitable precursors [74]. Since the precursors are usually in a liquid phase, these methods are mostly suitable for bioapplications. On the contrary, other methods are based on a thermodynamically induced self-aggregation of Si-nc in nonstoichiometric dielectrics [53]. It starts from an Si-rich oxide (SRO) film, which can be produced by deposition, sputtering, ion implantation, cluster evaporation, or sol-gel synthesis. The substochiometric SiO_x film is transformed into a composite film of Si-nc embedded SiO_2 by a partial phase separation mechanism, triggered by thermal annealing. The duration of the thermal treatment, the annealing temperature, and the Si excess content (Si_{exc}) in the SRO film determine the final size, size dispersion, and crystalline nature of Si-ncs. As a rule of thumb, greater silicon excess, higher annealing temperature, and longer annealing produce larger and more crystallized Si-ncs. The phase separation mechanism is also valid for the fabrication of Si-nc embedded in silicon nitride [75]–[77] and silicon carbide [78].

Generally, Si-ncs possess two remarkable PL features: high efficiency and tunable emission wavelength. And these features are direct consequences of quantum confinement effects. The emission band can be adjusted by simply changing the Si-nc size [53], while the improved efficiency has many causes. First, when the e-h wavefunctions are squeezed in real space due to the small size of the Si-nc, they broaden in momentum space, which causes a larger overlap of them and thus increases the radiative recombination probability (quasi-direct transitions) [79]. Secondly, the spatial constrictions of e-h pairs in Si-nc means that they are no longer free to diffuse as in bulk silicon, and thus the probability of finding nonradiative recombination centers is reduced significantly.

Thirdly, the decrease of the average refractive index of the material, an average value between those of Si-nc and SiO_2, increases the light extraction efficiency from the material itself by reducing the internal reflections.

So far, however, the physical origin of the PL property of Si-ncs is still under debate. The size dispersion of Si-ncs is usually claimed as the source of the broad emission line shape of the Si-nc emission spectra at room temperature. However, both size-selected deposition [80] and single Si-nc luminescence experiments [81] demonstrate that most of the luminescence broadening is intrinsic in nature, indicating that the PL spectrum has many contributions. In the Si-nc embedded SiO_2 system, the light emission is often characterized by a wide band in the wavelength range of 600–900 nm. This emission band red-shifts with the increase of the Si-nc mean size, which is qualitatively in agreement with the quantum confinement model and allows attributing this band to e-h recombination in Si-nc. Often, a second band, centered at 500 nm, can be observed. It is different from the Si-nc related band because it does not shift by changing crystallites' size. This band can be related to recombinations in matrix defects [82], which can be quenched by postgrowth annealing treatment, such as hydrogen passivation. There are other Si-nc and matrix interface defect-related luminescence bands that have been reported; interestingly, some of them depend on nanocrystal size [83]–[85].

It has been proposed that interface radiative states associated with oxygen atoms play a crucial role. They can be found either in the formation of silicon dimers [86] or in the form of $Si = O$ bonds [87] at the interface between the Si-nc and the oxide or within the oxide matrix. X-ray measurements and ab initio calculations [88] show the presence around the Si-nc of a strained SiO_2 region (about 1 nm) participating in the light emission process. The spatial distribution of the highest occupied and lowest unoccupied Kohn–Sham orbitals is totally confined in the Si-nc region with some weight on the interface O atoms, confirming the dot-nature of the near band-edge states but showing also the contribution of the surrounding SiO_2 shell. The calculation of the absorption spectrum shows that these new states originate strong features in the optical region, which can be at the origin of the PL observed for Si-nc immersed in a SiO_2 cage. Similar results have been obtained also by Monte Carlo simulations [84].

The role of the chemical passivation of the Si-nc has been pointed out in a recent experimental work [89], where the coupling between surface vibrations and fundamental gap as well as the increase of interaction between them in the strong confinement regime are proposed to interpret light emission. A recent study [90] shows that it is possible to switch between a quantum confinement nature of the emission to a recombination at defects by using hydrogen passivation: hydrogen passivates the defects and the PL is mainly due to quantum confinement effect, whereas ultraviolet illumination of the sample reactivates the defects, resulting in a defect-dominated emission. The understanding of the PL is even more complicated for Si-nc embedded in the silicon nitride system since more defect states and band tail states are involved [91], [92].

Achieving an efficient electrical injection and hence efficient Si-nc light-emitting devices (LEDs) has been the subject of several studies [93]–[95]. Interesting results have been obtained in ion implanted samples, showing maximum external quantum efficiency of about 3×10^{-5} [96]. Similar data have been obtained in plasma-enhanced chemical vapor deposition (PECVD) Si-nc [97]. Field-effect luminescence has been achieved by alternative injection of electrons and holes into Si-ncs with external quantum efficiencies of 0.03% [98].

Electrical injection into the Si-nc is a delicate task by itself. Different tunneling mechanisms in an Si-nc embedded SiO_2 film are reported schematically in Fig. 2. Indeed, in most of the reported devices, the EL is produced either by black-body radiation (the electrical power is converted into heat, which raises the sample temperature and then the device radiates) or by impact excitation of e-h pairs in the Si-nc by energetic electrons, which tunnel through the dielectric by, for example, a Fowler–Nordheim (F–N) process (see the left side of Fig. 2). Electron-hole pairs excited in this way recombine radiatively with an emission spectrum that is very similar to that obtained by PL. The problem with impact excitation and F–N tunneling is low efficiency and the damage to the oxide. To get high EL efficiency, one should try to get bipolar injection. However, bipolar injection is extremely difficult to achieve since the effective barrier for tunnelling of electrons is much smaller than that for holes. However, the bipolar injection can be easily achieved if direct tunneling occurs (see the right side of Fig. 2). Moreover, the voltage required for direct tunneling is usually lower than 3 V, whereas the voltage is higher than 3 V for F–N tunneling.

We have adopted an MOS device structure to optimize bipolar injection to Si-ncs [99], [100]. Fig. 3 shows the

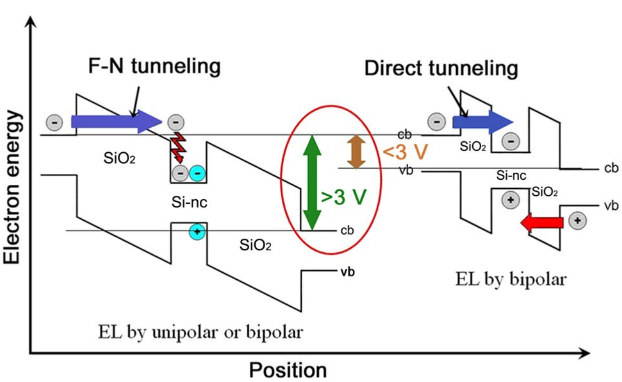

Fig. 2. *Schematic view of the process of generation of e-h pairs in silicon nanocrystals by impact excitation or direct tunneling: cb or vb refer to the conduction or valence band-edges.*

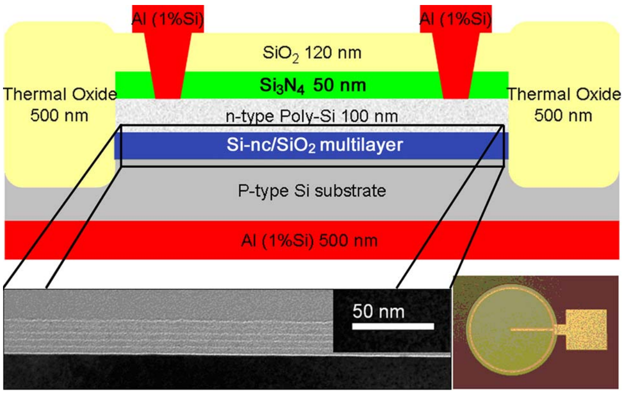

Fig. 3. ***(Top) Schematic cross-section and (bottom right) top view of the LED. (Bottom left) TEM image of the Si-nc/SiO_2 multilayer (annealed structure of 4 nm SRO/2 nm SiO_2 multilayer, five periods) [99], [100].***

schematic cross-section structure of an LED with Si-nc/ SiO_2 multilayer as active layer. A transmission electron microscope (TEM) cross-section image of the active layer is shown in the bottom left of Fig. 3. The top view of the LED is presented in the bottom right of Fig. 3. The active layer of the device is a multilayer structure composed of alternating Si-nc and SiO_2 layers on p-type silicon substrate. A 100-nm-thick n-type polycrystalline silicon (polysilicon) gate layer was deposited on the active layer, followed by deposition of an Al grid (500 nm thick). The metal-free region of the poly-Si layer has been covered by an antireflective coating (ARC; a 50-nm-thick Si_3N_4 layer and a 120-nm-thick SiO_2 layer).

The conductivity of the multilayer Si-nc LED is controlled by direct tunneling of electrical charges between Si-ncs [101]. Current–voltage (I–V) characteristics of such devices are shown in Fig. 4. The gate voltage means the voltage applied to the n-type polysilicon gate layer while the substrate is grounded (see Fig. 3). An I–V hysteresis loop was found, which is due to the charge accumulation or trapping in the device [100]. At these very low voltages, the current is due to the (inelastic) tunneling into the Si-nc/SiO_2 interface states [102]. The presence of the subbandgap interface states has been reported recently by us [103]. At higher voltages, the current has the same value under forward and reverse bias, which might indicate a bulk-limited nature of the measured current, controlled by the direct tunneling of electrical charges between the Si-ncs [104].

The current (voltage) values at which the EL signal was recorded are marked with the dots in Fig. 4. It is important to note that EL emission can occur at low voltages, lower than 3.2 V, corresponding to the height of the energy barriers at the silicon-oxide interface for electrons [105]. When high biases ($>$ 3.2 V) are applied, then F–N tunneling of electrons into silicon oxide conduction band occurs. So these observations indicate that direct tunneling of electrons and holes into the Si-nc is the predominant mechanism of excitation of EL in our devices under low biases. Moreover, the carrier injection is more efficient in sample with 4 nm SRO than that in sample with 3 nm SRO. This is due to the fact that the size and interdot distance of Si-ncs, key parameters for charge injection, depend on SRO thickness. Very weak EL emission was observed under reverse bias, which could be explain by the fact that hole tunneling current is negligible under reverse bias and the conduction band electron current is dominant over the entire voltage range [106].

The direct tunneling is not only less destructive than the F–N tunneling but also presents a more efficient way of injecting charges into the nanocrystals. This is evident from Fig. 5, which compares two Si-nc LEDs: multilayer

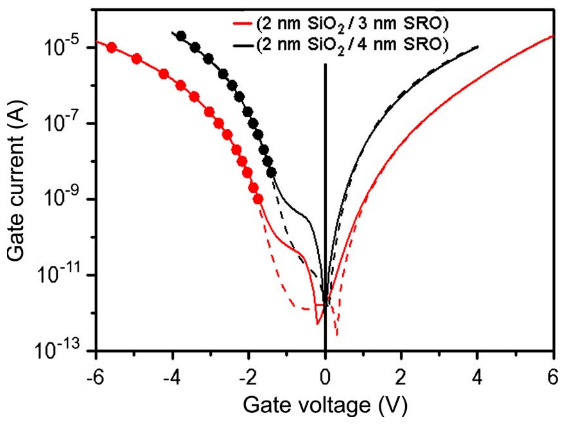

Fig. 4. ***Current-voltage characteristics of Si-nc/SiO_2 multilayer LEDs. The dots indicate the gate voltages (currents) at which EL signal was recorded. Very weak EL emission was observed under a high reverse bias and no emission when the bias was at the hysteresis loop region.***

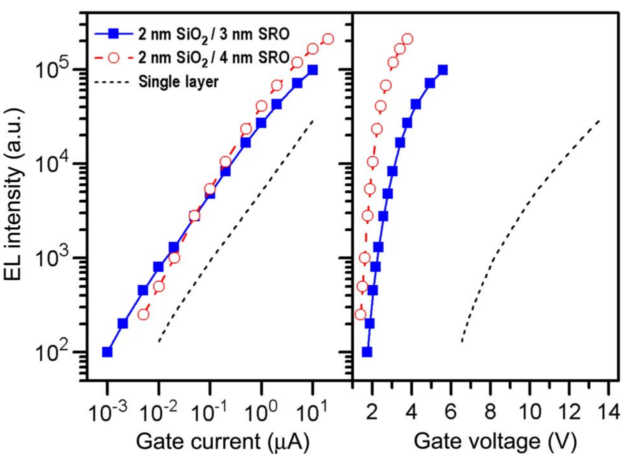

Fig. 5. ***Total EL intensity as a function of injected current and gate voltage. The dotted line is the corresponding EL emission from a LED with single layer as the active layer (~50 nm thick), which has the same composition as the SRO layer of multilayer LEDs.***

LEDs with the dominant direct tunneling and single-layer LED with the dominant F–N tunneling. This figure also shows a typical dependence of EL emission intensity on the injected current, which is a linear function in bi-log coordinates.

V. STATE OF THE ART ON THE WAY TO MAKING AN INJECTION LASER BY USING Si-nc

Here we show that Si-nc is itself an active laser material at visible wavelengths and the way that it can efficiently sensitize Er ions for light amplification in the infrared (IR) region.

A. Optical Gain in Si-nc (Visible Range)

Optically pumped gain in Si-nc thin films has been reported by several research groups, including us [10], [107], [108]. We have shown amplified spontaneous emission (ASE) from Si-ncs grown by different techniques (PECVD, superlattices, magnetron sputtering) and by means of the variable stripe length (VSL) technique in the CW and time-resolved (TR) regime, where the luminescence of Si-nc is used as a probe beam and one looks for enhancement as it propagates in an optically pumped waveguide. Fig. 6 shows representative results on Si-nc samples prepared by PECVD method. Loss or gain depends on the pump power and pumping length [Fig. 6(a)], which can be measured by the VSL technique [a schematic setup of the method is shown in the inset of Fig. 6(b)]. The TR ASE for various values of pump power and excited volume is shown in Fig. 6(b). By modeling the system within a one-dimensional amplifier scheme, the gain spectrum can be obtained. A summary of the emission, absorption, and gain spectra for a representative Si-nc sample is shown in Fig. 6(c). Absorption increases strongly at short wavelengths while emission (both spontaneous and stimulated) occurs at long wavelength. This is also called the Stokes shift between absorption and emission and is a characteristic of Si-nc. At the same time, the gain and luminescence spectra peak at different wavelengths, which indicates that either only the small Si-nc have strong gain or gain and luminescence have different origins. In the TR ASE spectra obtained by the VSL method, a fast recombination component appears in the decay dynamics [Fig. 6(b)], which disappears when either the excitation length l is decreased at a fixed pump density power (J_{pump}) or when J_{pump} is decreased for a fixed l. These observations rule out the nonradiative Auger processes as the origin of the observed fast component, since the intensity does not depend on l, whereas the fast recombination peaks are critically dependent on the pumping length, keeping fixed the excitation conditions.

The gain has also been observed in signal amplification (i.e., pump and probe) experiments [Fig. 6(d) and (e)]. A red signal beam is transmitted through a thin (200 nm) layer of Si-nc on a quartz substrate and, at the same time, a blue pump beam is exciting the Si-nc. When the power density of the pump beam is weak, the transmission though the Si-nc is mostly unaffected by the presence of the pump beam. On the contrary, when the pump power density is increased enough, the transmission through Si-ncs gets larger than unity. This means that the pump beam drives the Si-nc to the condition of population inversion where positive optical gain is observed.

Although a full theoretical model of the stimulated emission process in Si-nc is still lacking and the observed characteristics cannot be explained only on the basis of electron localization in the nanocrystals, a model to explain all these phenomena has been proposed, as shown in Fig. 7. The gain is associated with a four-level system, which can treat qualitatively the strong competition among losses, Auger recombinations, and stimulated emissions on the basis of rate equations of the relaxation dynamics [Fig. 7(a)]. In Fig. 7(b), absorption of a photon occurs as a vertical electronic transition between the ground state (level 1) and the excited state (level 2) of Si-nc. The excited cluster then relaxes to a new minimum energy configuration (level 3). Emission (either stimulated or spontaneous) is represented in this diagram by a downward electronic vertical transition to the level 4. Once the Si-nc is in its ground state, it relaxes again to the minimum energy configuration, which corresponds to level 1. Thus, by considering this interplay between ground and excited configurations, we find four levels associated with the absorption and emission processes. Note that this scheme implies that absorption (transition between level 1 and 2) occurs at shorter wavelengths than those of emission (transition between level 3 and 4) as observed experimentally. It is also worth noting that strong lattice relaxation (bond deformation) occurs when the Si-nc is excited.

One important characteristic of the optical gain in Si-ncs is the fact that stimulated emission occurs at a very fast (nanosecond) rate. This is a consequence of the delicate balance among stimulated emission and other nonradiative recombination processes, which quickly deplete the population inversion in Si-ncs. The typical lifetimes associated with these processes are [108]

$$\tau_{se} = \frac{4}{3}\pi R_{NS}^3 \frac{1}{\xi \sigma_g c n_{ph}}$$
$$\tau_A = \frac{1}{2C_A N_3}$$
$$\tau_{CC} = \frac{1}{2C_{CC} N_3}$$

where τ_{se}, τ_A, and τ_{cc} are lifetime of stimulated emission, nonradiative Auger, and free-carrier absorption, respectively. R_{NS} is the Si-nc radius, ξ the Si-nc packaging density, σ_g the emission cross-section, n_{ph} the photon flux

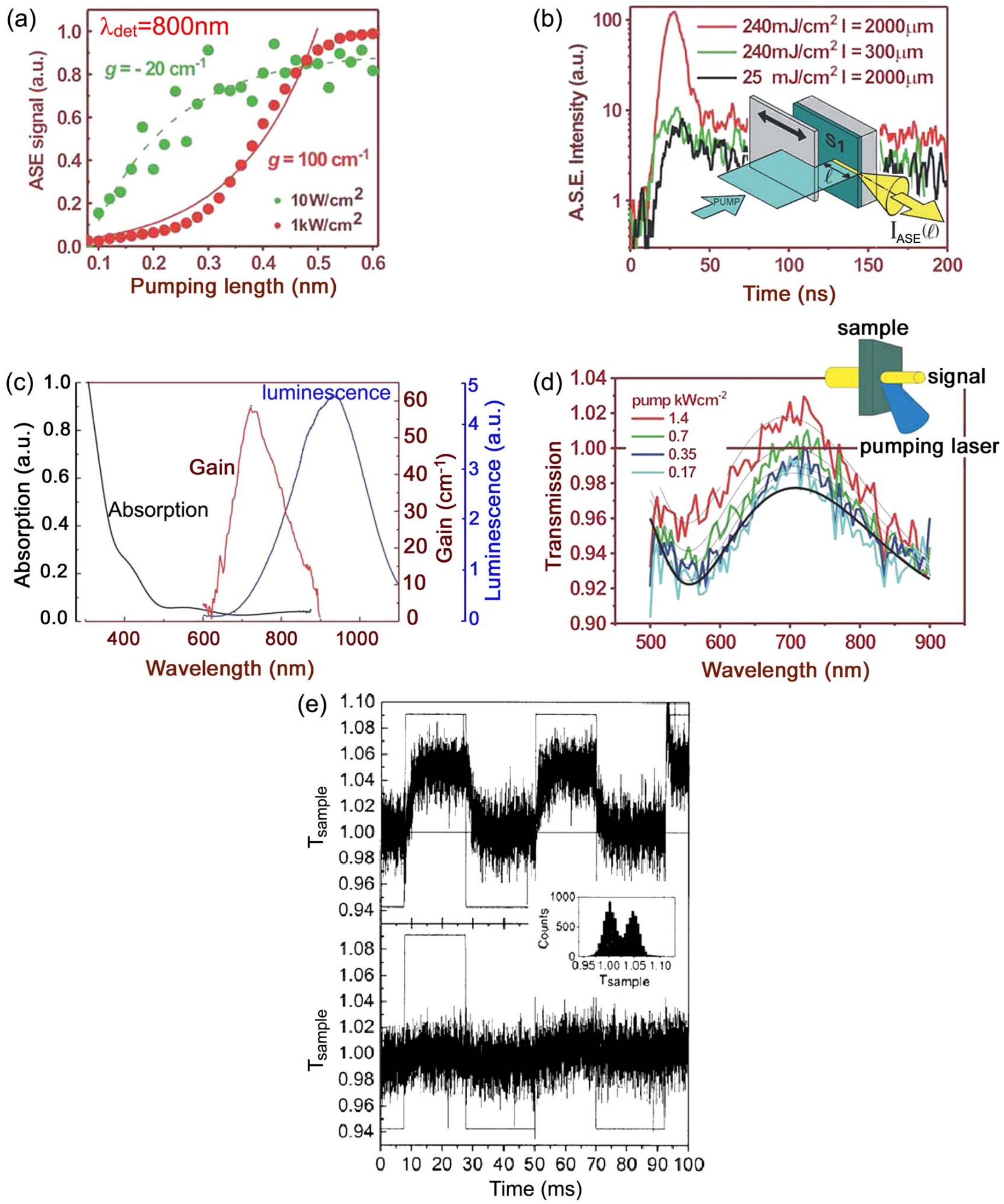

Fig. 6. ***(a) ASE versus the pumping length for two pumping powers at 800 nm. (b) TR ASE for various pump powers and excited volumes. The inset shows a scheme of the VSL method. (c) Summary of the optical properties of Si-ncs. (d) Transmitted intensity versus the wavelength for different power densities by pump and probe measurements. The dark line refers to the transmission of the sample without pump. The inset shows the scheme of the experiment. (e) Pump and probe experiments with chopped probe signal at (top panel) 2 kW/cm^2 and (bottom panel) 50 W/cm^2 pump intensity.***

density, C_A the Auger coefficient, N_3 the population density in the metastable level 3, and C_{CC} the excited carrier coefficient. It is clear that to have optical gain, τ_{se} must be smaller than τ_A and τ_{cc}. Since various parameters are strongly sample and configuration dependent, this tradeoff explains the difficulty in obtaining high optical gain in a systematic manner in Si-ncs.

B. Er-Doped Si-nc Amplifiers (IR Range)

Erbium-doped fiber amplifiers (EDFAs) are well established in long-haul transmission. However, there are difficulties, such as ion pair interactions and the small excitation cross-section of the Er ion, in reducing the size and cost of EDFA devices for widespread integration. In fact, EDFA devices are based on long and lightly doped

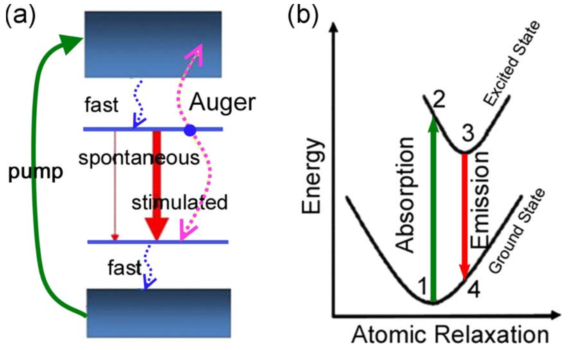

Fig. 7. ***(a) Energy diagram for a four level system. The various transitions are indicated by different lines; those with wavy lines are nonradiative. (b) Configuration coordinate diagram associated with atomic relaxation.***

fibers where high-power laser diodes are used as a pump. Clearly, a breakthrough would be a new gain medium that enables broadband optical or electrical excitation of rare-earth ions [109], with a potential of hundredfold reduction in pump costs. In addition, the new gain medium could provide order-of-magnitude enhancements in effective absorption cross-sections, with corresponding reductions of amplifier length dimensions. An Er-doped waveguide amplifier (EDWA) with an Si-nc based waveguide can be a candidate. First, Si-ncs have broadband optical absorption spectra, which mainly depend on the average size of the Si-nc and which are appreciable near 600 nm growing towards shorter wavelengths. Secondly, the absorption cross-sections of Si-ncs are on the order of 10^{-16} cm^2 in the 488 nm region, which is five orders of magnitude higher than that of Er^{3+} in stoichiometric silica [110], [111]. This value is also conserved when Si-nc is excited by electrical injection. Thirdly, the pump laser can be a high-power LED or, even, an electrical excitation circuit [112]. Fourthly, it has been demonstrated that Er^{3+}-doped silica containing Si-nc exhibits a strong energy coupling between Si-nc and Er^{3+}. Quantum efficiencies greater than 60% and fast (100 ns) Si-nc to Er^{3+} transfer rates have been measured. Moreover, in addition to the increase of effective excitation cross section (σ_{exc}) of the indirectly excited, Si-ncs increase the average refractive index of the dielectric matrix, allowing good light confinement and high electrical current, which opens the route to electrically pumped optical amplifiers.

Let us first summarize various mechanisms, although some of them are still controversial, and define the related cross sections for the Si-nc and Er^{3+} interaction system, as shown in Fig. 8. The excitation of Er^{3+} occurs via an energy transfer from e-h pairs that are photoexcited in the Si-nc: the overall efficiency of light generation at 1.535 μm from Er^{3+} through direct absorption in the Si-nc is described by an effective Er^{3+} excitation cross-section (σ_{exc}). On the other hand, the direct absorption of the Er^{3+} ion and the direct emission from the Er ions, without the mediation of the Si-nc, are described by absorption (σ_{abs}) and emission (σ_{em}) cross-section, respectively. The typical radiative lifetime of Er^{3+} is about 9 ms, which is similar to that of Er^{3+} in pure SiO_2. Several authors have suggested different channels for quenching of the Er^{3+} emission such as cooperative up-conversion [113], excited state absorption (ESA) [114], and Auger de-excitation [115]. We can see that, to optimize the system and achieve net optical gain in the amplifier, these detrimental processes must be avoided or reduced. More importantly, carrier absorption (CA) losses and the low number of Er^{3+} ions coupled to Si-nc (few percent) are main obstacles to achieving net optical amplification in Si-nc based EDWA. As for the former, a faster exciton recombination in small nanocrystals and/or faster carrier population depletion (due, for example, to a transfer mechanism) can reduce CA [116] because CA induced losses are proportional to the exciton population density in Si-nc. As for the latter, several reports revealed what seemed to be an intrinsic limit of the material itself [107], [117], [118].

A few groups have performed pump and probe measurements to look for optical amplification. The most successful result of 7dB/cm has been reported [18], where a very low Si-nc concentration was used. A successful experiment of top pumping with a 470 nm LED array was also reported, showing full inversion with maximum gain of 3 dB/cm [119]. In our laboratory, cosputtered samples [120] have been integrated into 10-μm-wide rib-loaded waveguides, as can be seen in Fig. 9. The scanning electron microscope (SEM) image of the waveguide is shown in the inset of Fig. 9. We infer an absorption loss coefficient at 1535 nm of about 4 dB/cm, while material losses at 1600 nm (out of absorption spectrum of Er ions) have been assessed about 1–2 dB/cm by the shift excitation spot technique [117]. We roughly estimate the percent of Er^{3+} coupled to Si-nc in our system to be 25% of optically active Er ions. This represents by far the largest improvement from a few percent reported in previous literature. The Auger back-transfer possibility was studied by using fast (nanosecond) TR IR

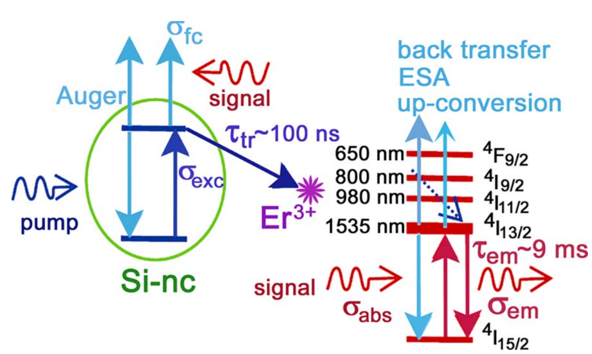

Fig. 8. ***Diagram of the excitation process of Er^{3+} ions via an Si-nc, with the main related cross-sections.***

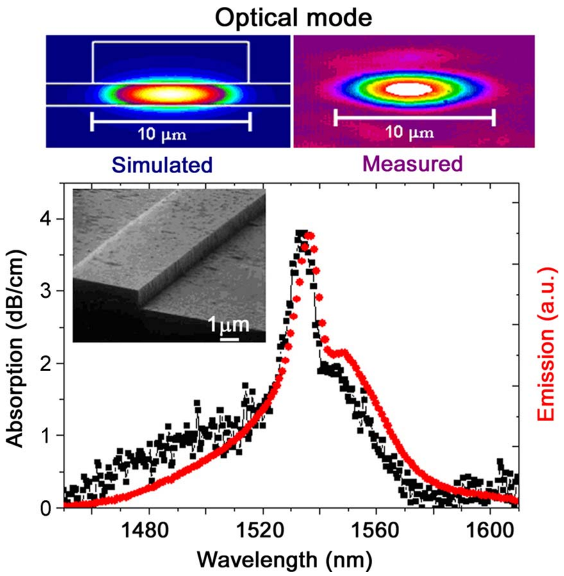

Fig. 9. *(Bottom) Absorption and emission spectrum of a Si-nc and Er^{3+} ions coupled rib waveguide (SEM picture in the inset) and (top left) simulated and (top right) measured output optical mode.*

spectroscopic measurements in our group. This combination of fast temporal and spectral analysis allowed us to separate different contributions to the PL signal. We found that the fast PL signal is associated with amorphous Si-nc or defects in the matrix, while only the slow one is characteristic of Er^{3+}. Moreover, no sign of Auger back-transfer has been detected. This allows us to conclude that the coupling among Si-nc and Er^{3+} is only ruled by geometrical effects [104] and that Auger back-transfer is not a real issue in high-quality samples.

VI. OTHER APPLICATIONS OF Si-nc IN SILICON PHOTONICS DEVICES

In this section, we will address applications of Si-nc in waveguides, optical resonant microcavities, and solar cells. The nonlinear optical property of Si-nc is also summarized. We will review recent results from our group [121] and make a comparison with the state of the art in each field.

A. Waveguides

Si-nc embedded SiO_2 has tunable refractive indexes [122] that are higher than that of SiO_2 (1.45). Therefore, it may have the advantage to form the core region of waveguides where the cladding is made of SiO_2. In these waveguides, optical losses can have different origins, both intrinsic [absorption, excited carrier absorption (ECA), Mie scattering] and extrinsic (scattering losses due to imperfections, sidewall scattering, radiation into the substrate). Optical losses of 120–160 dB/cm have been reported in the visible range [123], [124]. Lower values (about 10 dB/cm) have been reported for thick slab waveguides at 780 nm and $\sim$3.5 dB/cm at 1000 nm, where Rayleigh scattering is decreased according to the well-known $1/\lambda^6$ law [125]. Recently, optical loss as a function of the probe wavelength has been investigated [126]. Results show that propagation losses decrease with increasing the wavelength, from about 73 dB/cm (at 785 nm) to 2 dB/cm (at 1630 nm). Also, the absorption cross-section is about 3.5×10^{-18} cm^2 at 830 nm, increasing with decreasing wavelength.

In addition to linear losses, nonlinear optical losses are significant in Si-nc waveguides when using IR light. In Section VI-D, we will discuss the nonlinear absorption due to two photon absorptions. Here we will discuss ECA. Free-carrier absorption has been extensively studied in bulk silicon [127], while few works deal with that in Si-nc [128], [129]. An extensive study of the ECA mechanism in multilayer Si-nc rib waveguides has been reported [130]. A pump (532 nm) and probe (1535 nm) technique was used to assess the loss. The ECA loss coefficient can be written as a function of signal enhancement (SE), the ratio between the transmitted signal when the waveguide is pumped to the one when the waveguide is not pumped, in the following way:

$$\sigma_{\rm CA} N_{\rm Carr} = -\frac{\ln(\rm SE)}{\Gamma L_{\rm pump}}$$

where Γ is the optical mode confinement factor and $L_{\rm pump}$ is the length of the waveguide that is actually excited by the pump; $N_{\rm Carr}$ is the number of excited carriers and $\sigma_{\rm CA}$ is the absorption cross-section of the waveguide at the signal wavelength.

In Fig. 10(a), the transmitted signal is shown when the pump is switched on. A rapid decrease in the transmission is observed. The dynamics of the decrease is characterized by two time scales: one fast (order of microseconds) and one slow (order of seconds). The slow one is due to thermal effects while the other is due to ECA. Fig. 10(b) shows the maximum of the ECA loss as a function of the pump photon flux $\Phi_{\rm p}$. ECA losses increase with $\Phi_{\rm p}$, up to 6 dB/cm for $\Phi_{\rm p} = 3 \times 10^{20}$ ph/cm^2s. A square root dependence of $\sigma_{\rm CA} N_{\rm Carr}$ on $\Phi_{\rm p}$ is observed. Since $\sigma_{\rm CA}$ is independent of $\Phi_{\rm p}$, so $N_{\rm Carr}$ depends on $\Phi_{\rm p}^{1/2}$. This is an indication of Auger dominated recombination processes in the Si-nc, possibly between adjacent Si-ncs due to their particular close distribution in multilayer samples. If we assume one excited carrier per Si-nc at high pumping rate from $\sigma_{\rm CA} N_{\rm Carr} = 1.4$ cm^{-1}, we get $\sigma_{\rm CA} = 4 \times 10^{-19}$ cm^2 at 1535 nm, when $N_{\rm Carr} = 3.5 \times 10^{18}$ cm^{-3}. In addition, the ECA has the same characteristic dynamics of the recombination of exciton luminescence in large Si-nc [see the inset of Fig. 10(b)]. This indicates that the way to reduce the excited carrier absorption is to decrease the Si-nc size in the waveguide.

As Si-nc embedded SiO_2 has a relatively low refraction index, its application in conventional stripe waveguides would result in a large cross-section and weak light confinement. So, a new waveguide architecture, the slot waveguide [19], has been proposed, which uses the electric-field discontinuity at the interfaces between different dielectric materials and where light propagates mostly in the low index medium. This kind of device is often designed as a sandwich-like structure with the low index medium in the center. Due to the high index contrast, modes with strong field intensity at the two low/high index medium interfaces of the slot are formed. The overlap of the evanescent tail of the modes in the central slot leads to a strong light confinement in the low index region. Examples of such structures are shown schematically in Fig. 11: an SRO slot (100–150 nm) sandwiched by two silicon waveguides (width of 500 nm and height of 200–300 nm) [131]. Both vertical [Fig. 11(a)] and horizontal [Fig. 11(b)] configurations have been proposed. The vertical approach has some difficulties for fabrication since it is difficult for the standard technique to fill the slot with SRO, while the horizontal or sandwich slot structure allows one to overcome this problem and to fulfill the tight requirements for mass production. These slot waveguides show propagation loss as low as 4 dB/cm at 1550 nm.

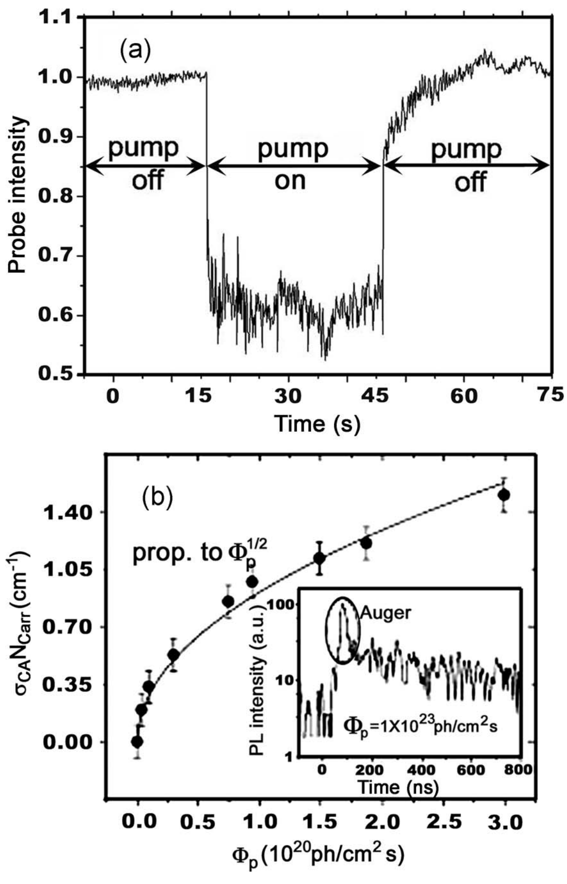

Fig. 10. *Direct measurement of the intensity of a 1535 nm signal for different pump photon fluxes: (a) full temporal dynamics and (b) carrier absorption losses of 1535 nm signal as a function of the photon flux. A square root fit to the experimental data is also shown (solid line) [130].*

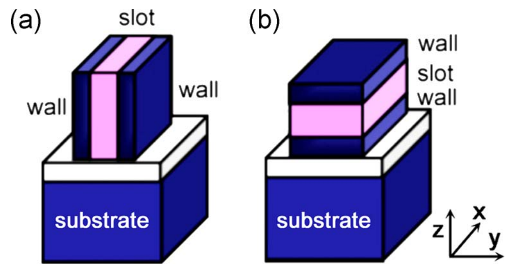

Fig. 11. *Schematic structures of (a) vertical and (b) horizontal slot waveguides. The light propagates in the x-direction.*

B. Optical Resonant Microcavities

In the past few years, a series of achievements has been made in the fabrication of optical micro- and nanocavities [132], where the light is confined in a small modal volume by resonant recirculation with low round-trip optical loss. Such optical structures are used to achieve lasing action: as an example, Er-doped microspheres and microtoroids were realized [133]. However, the disadvantage of these devices is that they are not planar, making them difficult to incorporate into CMOS technology. Therefore, planar optical cavities, such as ring resonators or photonic crystal waveguides, as well as "traditional" linear optical resonators, such as Fabry–Perot and distributed feedback cavities, are preferred for CMOS compatibility.

In the following, we will provide a brief assessment of the main optical properties of microcavities enhanced by Si-ncs. In particular, the application of Si-ncs in slow wave structures is worth noting.

1) Ring Resonators: Ring resonators (RRs) are versatile building blocks with various applications, from telecommunication and sensing to basic scientific research. They are also widely used in photonics to shrink the size of modulators and to route the light and allow high-speed optical buffering [134]. In a common RR layout, a light beam travels through a waveguide in close proximity to a ring, so that the evanescent fields of the optical modes overlap, and optical energy transferred to the ring and back to the waveguide may occur. The strength of the coupling in the RR can be controlled by adjusting the gap distance between the waveguide and the ring. The smaller the gap, the larger the coupling efficiency.

A resonance requires that the optical path length in the ring be a multiple of the wavelength of the input photons, or $m\lambda_m = 2\pi R\, n_{eff}$, where R is the ring radius, n_{eff} is the effective refractive index of the waveguide, λ_m is the resonance wavelength, and m is an arbitrary integer. A change in R or n_{eff} would shift the resonant wavelength.

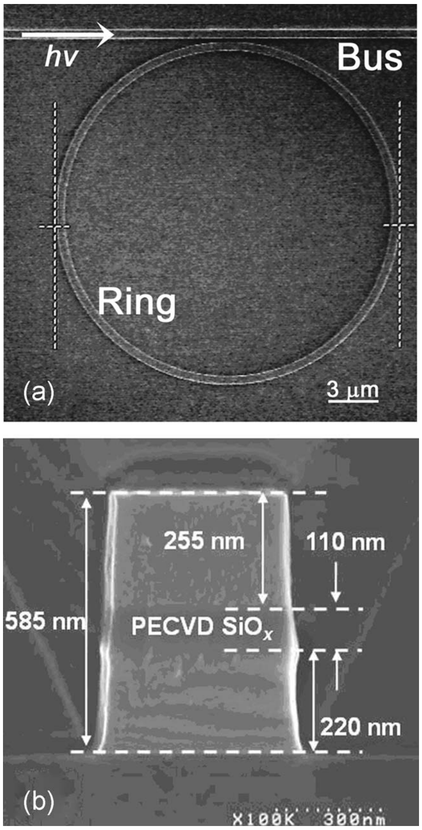

Fig. 12. ***(a) SEM top view image of an RR coupled to a bus waveguide and (b) cross-sectional TEM view of the horizontal slot waveguide structure.***

The cavity field enhancement effect is also an important characteristic in such devices, which makes it possible to build up the intensity inside resonators.

The confinement could be enhanced if we introduce Si-nc into the waveguide and the ring. Such a device has been fabricated, as shown in Fig. 12. Also, the horizontal slot waveguide is adopted. These can be used to enhance the nonlinear interaction in the arms of a Mach–Zehnder interferometer and reduce the power threshold to induce a refractive index variation, for switching applications. The ring radius has been varied from 10 to 40 μm and the resonant wavelength is changed accordingly. The highest quality factor (Q) has been found in a sample with a gap distance of 250 nm and a ring radius of 20 μm. Large Q factors allow using these systems for active all-optical devices based on Si-nc [135].

2) Slow Wave Devices: The slow wave phenomenon, reducing the speed of light during its propagation, can enhance nonlinear effects. In principle, slow wave structures can be implemented in several ways, such as coupled cavities in photonic crystals, coupled ring microresonators, stacks of dielectric disks, etc., since the existence of evenly spaced strongly confined cavities is the unique requirement [136]. Slow wave technology is nowadays widely used in various devices such as optical fibers [137] and photonic crystals [138]. In waveguide technology, coupled resonator optical waveguides (CROWs) are used [136], where the group velocity of the photons resonant with the cavity optical modes can be controlled by adjusting the spacing between consecutive cavities, effectively "slowing" or "storing" light within the device for a longer time. With this kind of device, a delay as high as 500 ps has been demonstrated [139]. One such device is consecutive cavity waveguide (CCW), where the main advantage is that the central frequency region of the CCW guided mode is dispersionless. On the other hand, the main drawback is that a CCW is inherently lossy in the dispersionless region, although low losses can be obtained by a proper design of the CCW. A recent approach is the realization of slow wave devices based on slot waveguide structures, in which the group velocity of light can be controlled and, at the same time, the electric field can be localized in the low index slotted material. Structures based on photonic crystals waveguides [140] and channel waveguides [141], [142] have been designed and realized.

To exploit the slow wave effect in Si-nc waveguides, a CROW-based slot waveguide working at 1.55 μm has been designed [141]. For the horizontal configuration, the optimum system consists of a one-dimensional photonic crystal formed by air-slabs. The SEM top-view image of the device consisting of one cavity between two Bragg mirrors and its cross-section illustration are shown in Fig. 13(a) [142]. It can be seen that the device is composed of one SRO layer sandwiched by two silicon layers. Moreover, the distance and the cavity length can be adjusted to optimize the slow wave effect. The measured transmission spectra of such a device in quasi-TM polarization and normalized to the wavelength in the center of the optical bandgap can be seen in Fig. 13(b). It is possible to recognize the bandgap and the Bloch mode peak for the wavelength resonant with the cavities mode. The spectra simulated with a three-dimensional finite-difference time-domain (3D-FDTD) algorithm are shown in Fig. 13(c). A shift of about 100 nm is present between the simulated and experimental data due to a difference between the nominal and real photonic structure. Nevertheless, the spectral features of the photonic gap are quite similar. Since the coupling between the cavities is not strong enough, it is not possible to resolve the five different cavity peaks, which appear as a single, broadened peak, clearly visible around 1.5 μm in Fig. 13(b) and (c). The measured extinction rate of the stop band is more than 15 dB. Although the results are still preliminary, such photonic structures seem very promising to get efficient slow wave photonic linear waveguides based on Si-ncs.

3) Microdisk Resonators: The microdisk resonator is a kind of optical device that produces optical modes called whispering gallery modes (WGMs) [143], which are circularly propagating optical modes suffering continuous total internal reflection inside the resonator. Optically passive microdisks, based on transparent materials with negligible absorption losses, have high Q factors (10^6–10^{10}), while active resonator systems, such as III–V semiconductor quantum dot microdisk lasers, report active Q factors of 10^3–10^4 in the visible and near IR wavelength range [144], [145]. Such high-Q cavities can be employed in a wide range of applications, like frequency comb generators [146], optomechanics [147], and environmental sensors [148]. Lately, they are widely used as experimental platforms to study fundamental physics of cavity-quantum electrodynamics [149].

So far, only a few works on Si-nc based microdisks have been published, where Q factors of a few hundred have been reported [132], [150]. It has been reported [151] that Si-nc embedded SiO_2 film microdisks were fabricated on top of an Si wafer. Then the wafers were photolithographically patterned and dry-etched anisotropically to form arrays of microdisks with diameters ranging from 2 to 10 μm. The crystalline wafer was finally wet-etched isotropically to form the mushroom-like microdisks, as can been seen in Fig. 14(a). The PL signal of a single microdisk was collected in its plane and the WGM emission observed.

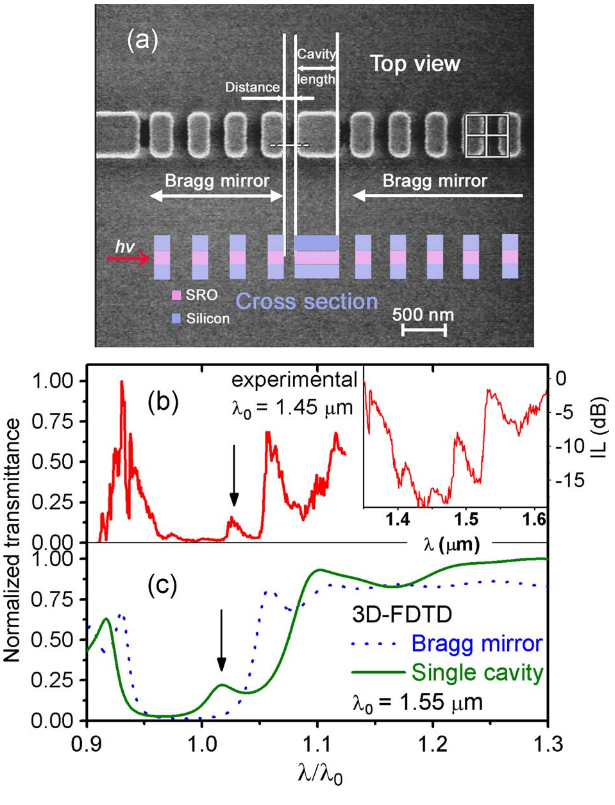

Fig. 13. ***(a) Scheme and SEM image of the photonic crystal structure processed on a horizontal slot waveguide (top view). Inset: schematic cross-section of the device. (b) Experimental measurement of the coupled resonance optical waveguide structure ($\lambda_0 = 1.45$ μm) for quasi-TM polarized light. The arrow shows the cavity peaks (inset-insertion losses of the device). (c) 3D-FDTD simulation of the device with a single cavity and the Bragg mirror ($\lambda_0 = 1.55$ μm).***

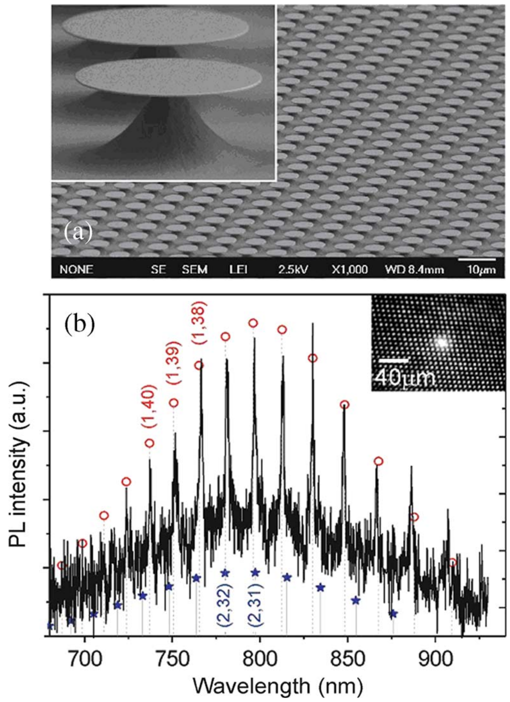

Fig. 14. ***(a) SEM images of the array and the single disk resonator. (b) Measured TE-polarized WGM spectrum of an 8 μm diameter microdisk is plotted together with the simulated peak positions for the first radial mode family (o). (Inset) The bright spot in the photograph is the direct image of the visible PL emission of Si-nc from a single disk resonator.***

In Fig. 14(b), one can observe the WGM structure of the single microdisk: subnanometer emission lines, corresponding to Q factors of almost 3×10^3. Both 3D-FDTD simulations and experimental results confirm that such thin microdisks do not support guided TM modes because of the very low effective index for this polarization ($n_{eff} = 1.08$). Thus, all the observed spectral peaks are TE-polarized and belong to the same radial family, with corresponding azimuthal mode numbers (m) extending from m = 42 (710.5 nm) to m = 29 (928 nm) and an average mode spacing of $\sim$15 nm.

Q values of a microdisk can be affected by pump power. Fig. 15 shows the dependence of the measured Q values of a thin microdisk on incident light pump power (P), where three distinct resonances at $\lambda = 754$, 768, and 849 nm (m = 39, 38, and 33, respectively) were used. It was found that the wavelength of incident light has limited effects on the Q factor, while the Q factor decreases as the pump power increases. This can be attributed to the fact that at high excitation powers, we either introduce an additional loss source or enhance the existing ones due to ECA. Thermal heating effects have been ruled out by the absence of a relative spectral shift of the resonances or a modification

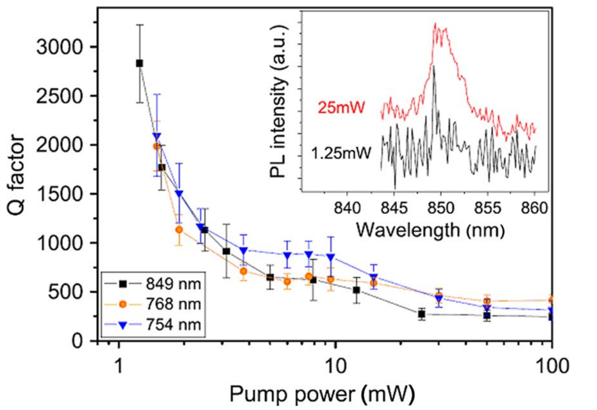

Fig. 15. ***The measured Q factors at increasing pump power are plotted at three different wavelengths, reporting an order of magnitude variation between two extreme pump powers. The inset shows the WGM mode at $\lambda = 849$ nm at two different pump powers.***

of the mode spacing [130]. Such absorption events will enhance the cavity losses, causing the observed WGM broadening. The situation gets more complicated when the spontaneous emission signal gets strong enough to affect the exciton population, as in the case of stimulated emission. When this becomes the dominant mechanism, one can expect that the absorption grows sublinearly with pump power (increasing transparency), leading to an inversion in the tendency of the Q-P curve (mode narrowing at high powers); hence, it would be possible to achieve net gain and eventual lasing at higher pump powers.

It should be pointed out that the observed Q factors can be further enhanced by the optimization of the SRO material. Microdisk resonators could hopefully allow for a low-threshold laser action even with the low inhomogeneously-broadened gain spectrum of Si-nc in a similar way as in III–V semiconductor microdisk devices.

C. Solar Cells

Recent results have shown the possibility of using Si-nc to develop third generation photovoltaics [152], [153], where the theoretical efficiency is well beyond the Shockley–Quiesser efficiency limit [154]. There are many applications of Si-nc in solar cells. One of them is the all-silicon tandem cell [155], where the Si-nc has larger and tunable bandgap than bulk silicon and can absorb more efficiently the photons with high energy. The other is the hot carrier solar cell [105], where photoexcited carriers with high energy (hot carrier) can be collected while they are still at elevated energies and thus allowing higher voltages to be achieved. Ideally this collection would be isoentropic using monoenergetic contact, which has been attempted experimentally by a structure with a single layer of Si-nc sandwiched by SiO_2 [156].

All-silicon tandem cell is mostly fabricated by a superlattice approach, where the phase separation is the main mechanism to fabricate Si-ncs [80]. For solar cell applications, the main challenge for this structure is to achieve sufficient carrier mobility and hence a reasonable conductivity. This generally requires formation of a true superlattice with overlap of the wave function for adjacent quantum wells or quantum dots, which in turn requires either close spacing between Si-ncs or a low barrier height. That is to say that the inter Si-nc distance is more important than Si-nc size [157]. However, the transport can be affected by the matrix in which the Si-nc embedded. It has been found that SiC and Si_3N_4 matrices give lower barrier heights [105] and also longer distance between Si-ncs for significant wave function overlapping [158] than those of SiO_2. The conductivity can also been improved by using a lateral multilayer Si-nc/SiO_2 structure [159]. This means that the carrier extraction takes place parallel to the Si/SiO_2 interfaces of two-dimensional Si-ncs while growth confinement is sustained in the vertical direction. It was shown that the lateral contact scheme is able to provide four orders of magnitude enhanced conductivity compared to a Si-nc/SiO_2 multilayer with standard vertical contacts where the charge transport is limited by insulating SiO_2 barriers [160].

Another problem for this multilayer structure is the precise control of the Si-nc size by the thickness of SRO layer. It has been found that in Si-nc/SiO_2 multilayers, a crystallinity of ~5% for the 2-nm-thick and ~25% for the 5-nm-thick SRO layers was obtained [161]. This is mainly influenced by stress, which depends on the periods of the multilayer, substrate, and annealing processes [162].

Some interesting photoresponse features for photovoltaics of Si-nc embedded SiO_2 layers were also found. For example, multiple exciton generation [163]–[165] was recently reported in an MOS-like device, where the oxide is an Si-nc embedded silicon oxide. This will enhance the current in the solar cell. The device structure is shown in Fig. 16. A clear photovoltaic effect is observed with an open

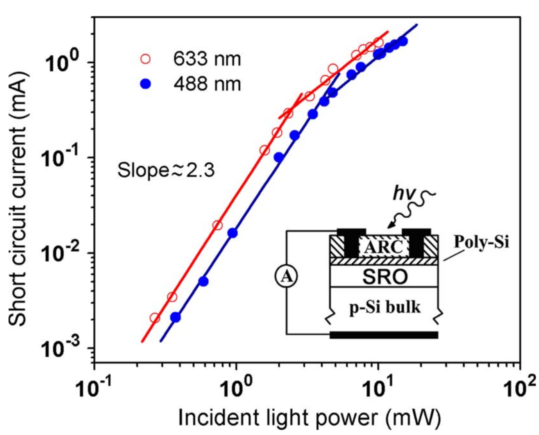

Fig. 16. ***Short circuit current as a function of incident light power for two different wavelengths. Inset: schematic cross-sectional structure of the device.***

circuit voltage of ~600 mV. This particular cell configuration is characterized by a small filling factor, which accounts for the low efficiency of the cell (~12%) [100], [103].

What is more relevant here is the observation of a superlinear photovoltaic effect at low light incident power. This is illustrated in Fig. 16, where the short circuit current increases according to a power law with exponent larger than two as a function of the incident power. It seems that for each photon, two or more electrons contribute to the current. Since the energy of the absorbed photon (633/488 nm) is much larger than the nanocrystal bandgap, the photogenerated electron has extra kinetic energy that can be released by impact excitation of the trapped electron at nitrogen-related midbandgap states [166], which was confirmed by the IR response. This mechanism generates a current of secondary carriers, which sum up to the photocurrent, and explains the super linear photovoltaic effects. In fact, with illumination of solely high energy photons, secondary carrier generation works as a mechanism that recovers electrons relaxed into the subbandgap states. When subbandgap excitons are generated directly by IR illumination, secondary carrier generation works as an amplification mechanism for the IR photocurrent component. For this reason, the adoption of SRO in silicon-based solar cells could offer the opportunity to exploit efficiently the subbandgap photons present in the solar spectrum.

D. Nonlinear Optical Properties of Si-nc

Injection-based devices, either based on the electro-optical effects or on free-carrier effects, do not seem suitable for power efficient high-speed optical networks (40 Gbps and beyond). Therefore, all-optical devices, where an optical signal traveling through a circuit is controlled by another external optical signal by means of nonlinear interaction in a Mach–Zehnder interferometer, are getting more and more attention. In such devices, nonlinear photonic materials are vital.

Different physical mechanisms like bound electrons, free carriers, and local heating can contribute to Si-nc optical nonlinearities, which are differentiated by their response time. The bound electronic response is very fast and involves a distortion by the optical field of the electronic cloud around an atom. Moreover, the electronic nonlinearity (n_{2be}) can be greatly enhanced if the atom is highly polarizable. Single- or two-photon absorption processes can excite free carriers in a semiconductor. In turn, these free carriers absorb the incident radiation and result in an effect that is related by Kramers–Kronig relation to a change of the refractive index. Thus the nonlinear refractive index (n_{2fr}) can be enhanced by excitation of a significant population via one- or two-photon absorption. The induced free-carrier refraction occurs on a time scale typical of carrier generation and their recombination, i.e., in a time scale of hundreds of microseconds. The thermalization of excited carriers via nonradiative recombination is responsible for the heating of the material and constitutes one of the sources of the thermal lensing effect (n_{2th}). Thus, the nonlinear index n_2 of a semiconductor is the result of three terms: $n_2 = n_{2be} + n_{2fr} + n_{2th}$.

Si-nc has a rich phenomenology for nonlinear applications. If one compares the results found for n_2 in Si-nc at 1550 nm [167] with the data of other materials such as silica [168], silicon [169], and GaAs [170], it can be found that Si-nc is as good as III–V materials in nonlinear applications, thus opening the route to all optical modulation.

The n_2 of Si-nc can be measured by using the nonlinear transmission z-scan method [171] with a 1550 nm pump laser. Results show that n_2 ranges from 10^{-9} to 10^{-8} cm^2/W and nonlinear absorption coefficient β varies from 10^{-7} to 10^{-6} cm/W, as the Si_{exc} increases up to 24 at.%. The obtained nonlinear coefficients are considerably high, leading to a nonlinear contribution to n_2 and β, which are comparable to the linear ones (n and α). On the other hand, the results of the z-scan measurements showed a change of the nonlinear refractive index when changing from nano- or picsosecond-long pulses to femtosecond short pulses, as depicted in Fig. 17. Also the magnitude of the nonlinear response changed. In fact, in the femtosecond regime, a positive nonlinear refractive index (valley-peak curve) on the order of $n_2 \sim 10^{-13}$ cm^2/W was detected for a peak intensity (I_p) in the range of 10^{11}–10^{12} W/ cm^2, which is due to the bound electronic response. In the picosecond excitation regime, a stronger negative nonlinear

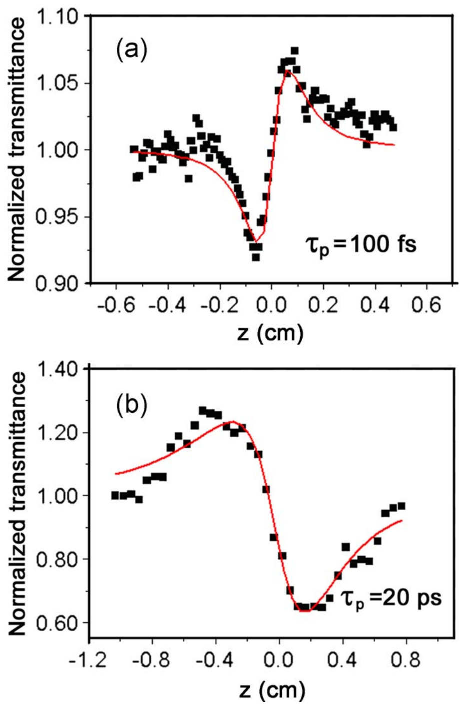

Fig. 17. *Comparison between z-scan measurements for (a) fast and low repetition rate exciting pulses and (b) high repetition rate exciting pulses on the sample with 21 at.% of Si_{exc} annealed at 800 °C.*

response (peak–valley curve) was detected on the order of $\sim 10^{-11}$ cm^2/W for $I_p = 10^9$–10^{10} W/cm^2. This negative nonlinear response is due to free-carrier refractive effects.

It was also found that the n_{2be} is a function of both the annealing temperature (T_{ann}) and Si_{exc}. In particular, a strong n_{2be} is obtained from the sample with low Si_{exc} and annealed at low T_{ann}. These parameters mean a small Si-nc size, and hence this is evidence of a quantum confinement effect. This has been proved by some experimental results [167], [172]. Moreover, a theoretical calculation shows that for Si-nc with a diameter smaller than 2 nm, the quantum confinement effect strongly enhances the nonlinear response of the system [173].

VII. CONCLUSION

As an enabling material for silicon photonics, Si-nc has proved its importance to a wide scope of photonic devices such as light emitters, waveguides, resonators, and solar cells. It has greatly improved the performance of these devices. However, there is still plenty of room to get Si-nc precisely controlled, device parameters optimized, and new phenomena discovered and utilized. Also, further breakthroughs can be foreseen in the near future with the investigation and demonstration of a wide spectrum of new photonic devices, in which Si-nc will continue to make key contributions. ■

Acknowledgment

The authors appreciate the help of many coworkers from both national and international collaborations. They can be recognized in the cited literature. The ongoing collaboration with the MTLab of FBK-irst has permitted the achievement of most of the results shown here. In particular, the authors would like to recognize the hard work of many present and past collaborators of the Nanoscience Laboratory without whom the research reported here would not have been performed and realized.

REFERENCES

[1] R. A. Soref and J. P. Lorenzo, "Single-crystal silicon—A new material for 1.3 and 1.6 μm integrated-optical components," *Electron. Lett.*, vol. 21, pp. 953–954, 1985.

[2] R. A. Soref and J. P. Lorenzo, "All-silicon active and passive guided-wave components for $\lambda = 1.3$ and 1.6 μm," *IEEE J. Quantum Electron.*, vol. 22, pp. 873–879, 1986.

[3] L. Pavesi and D. Lockwood, *Silicon Photonics: Topics in Applied Physics*. Berlin, Germany: Springer-Verlag, 2004, vol. 94.

[4] L. T. Canham, "Silicon quantum wire array fabrication by electrochemical and chemical dissolution of wafers," *Appl. Phys. Lett.*, vol. 57, pp. 1046–1048, 1990.

[5] R. A. Soref, "Silicon-based optoelectronics," *Proc. IEEE*, vol. 81, pp. 1687–1706, 1993.

[6] L. C. Kimerling, "Silicon microphotonics," *Appl. Surf. Sci.*, vol. 159–160, pp. 8–13, 2000.

[7] O. Bisi, S. U. Campisano, L. Pavesi, and F. Priolo, "Silicon based microphotonics: From basics to applications," in *Proc. E. Fermi Schools: Course CXLI*, Amsterdam, The Netherlands, 1999.

[8] F. Huang, K. Sakamoto, K. Wang, P. Trinh, and B. Jalali, "Epitaxial SiGeC waveguide photodetector grown on Si substrate with response in the 1.3–1.55 μm wavelength range," *IEEE Photon. Technol. Lett.*, vol. 9, pp. 229–231, 1997.

[9] L. Colace, G. Masini, and G. Assanto, "Ge-on-Si approach to the detection of near-infrared light," *IEEE J. Quantum Electron.*, vol. 35, pp. 1843–1852, 1999.

[10] L. Pavesi, L. Dal Negro, C. Mazzoleni, G. Franzo, and F. Priolo, "Optical gain in Si nanocrystals," *Nature*, vol. 408, pp. 440–444, 2000.

[11] G. Dehlinger, L. Diehl, U. Gennser, H. Sigg, J. Faist, K. Ensslin, D. Grutzmacher, and E. Muller, "Intersubband electroluminescence from silicon-based quantum cascade structures," *Science*, vol. 290, pp. 2277–2280, 2000.

[12] M. H. Nayfeh, N. Barry, J. Therrien, O. Akcakir, E. Gratton, and G. Belomoin, "Stimulated blue emission in reconstituted films of ultrasmall silicon nanoparticles," *Appl. Phys. Lett.*, vol. 78, pp. 1131–1133, 2001.

[13] O. Boyraz and B. Jalali, "Demonstration of a silicon Raman laser," *Opt. Express*, vol. 12, pp. 5269–5273, 2004.

[14] M. Chen, J. Yen, J. Li, J. Chang, S. Tsai, and C. Tsai, "Stimulated emission in a nanostructured silicon pn junction diode using current injection," *Appl. Phys. Lett.*, vol. 84, pp. 2163–2165, 2004.

[15] R. J. Walters, R. I. Bourianof, and H. Atwater, "Field-effect electroluminescence in silicon nanocrystals," *Nat. Mater.*, vol. 4, pp. 143–146, 2005.

[16] K. K. Lee, D. R. Lim, H.-C. Luan, A. Agarwal, J. Foresi, and L. C. Kimerling, "Effect of size and roughness on light transmission in a Si/SiO_2 waveguide: Experiments and model," *Appl. Phys. Lett.*, vol. 77, pp. 1617–1619, 2000.

[17] M. Loncar, T. Doll, J. Vuckovic, and A. Scherer, "Design and fabrication of silicon photonic crystal optical waveguides," *J. Lightw. Technol.*, vol. 18, pp. 1402–1411, 2000.

[18] H.-S. Han, S.-Y. Seo, and J. H. Shin, "Optical gain at 1.54 μm in erbium-doped silicon nanocluster sensitized waveguide," *J. Appl. Phys.*, vol. 27, pp. 4568–4570, 2001.

[19] V. Almeida, Q. Xu, C. Barrios, and M. Lipson, "Guiding and confining light in void nanostructure," *Opt. Lett.*, vol. 29, pp. 1209–1211, 2004.

[20] E. Kuramochi, M. Notomi, S. Hughes, A. Shinya, T. Watanabe, and L. Ramunno, "Disorder-induced scattering loss of line-defect waveguides in photonic crystal slabs," *Phys. Rev. B*, vol. 72, p. 161318, 2005.

[21] Y. A. Vlasov, M. O'Boyle, H. F. Hamann, and S. J. McNab, "Active control of slow light on a chip with photonic crystal waveguides," *Nature*, vol. 438, pp. 65–69, 2005.

[22] C. E. Png, G. T. Reed, R. M. H. Atta, G. J. Ensell, and A. G. R. Evans, "Development of small silicon modulators in silicon-on-insulator (SOI)," in *Proc. SPIE*, 2003, vol. 4997, pp. 190–197.

[23] Y.-H. Kuo, Y.-K. Lee, Y. Ge, S. Ren, J. E. Roth, T. I. Kamins, D. A. B. Miller, and J. S. Harris, "Strong quantum-confined Stark effect in germanium quantum-well structures on silicon," *Nature*, vol. 437, pp. 1334–1336, 2005.

[24] Y. Akahane, T. Asano, B. S. Song, and S. Noda, "High-Q photonic nanocavity in a two-dimensional photonic crystal," *Nature*, vol. 425, pp. 944–947, 2003.

[25] Q. Xu, B. Schmidt, S. Pradhan, and M. Lipson, "Micrometre-scale silicon electro-optic modulator," *Nature*, vol. 435, pp. 325–327, 2005.

[26] B. S. Song, S. Noda, T. Asano, and Y. Akahane, "Ultra-high-Q photonic double-heterostructure nanocavity," *Nat. Mater.*, vol. 4, pp. 207–210, 2005.

[27] M. Jutzi, M. Berroth, G. Wohl, M. Oehme, and E. Kasper, "Ge-on-Si vertical incidence photodiodes with 39-GHz bandwidth," *IEEE Photon. Technol. Lett.*, vol. 17, pp. 1510–1512, 2005.

[28] J. Michel, J. F. Liu, W. Giziewicz, D. Pan, K. Wada, D. D. Cannon, S. Jongthammanurak, D. T. Danielson, L. C. Kimerling, J. Chen, F. O. Ilday, F. X. Kartner, and J. Yasaitis, "High performance Ge p-i-n photodetectors on Si," in *Proc. Group IV Photon. Conf.*, 2005, pp. 177–179.

[29] B. Jalali, "Silicon Photonics," *J. Lightw. Technol.*, vol. 24, pp. 4600–4615, 2006.

[30] R. A. Soref, "The past, present, and future of silicon photonics," *IEEE J. Sel. Topics Quantum Electron.*, vol. 12, p. 1678, 2006.

[31] M. E. Castagna, S. Coffa, M. Monaco, A. Muscara, L. Caristia, S. Lorenti, and A. Messina, "High efficiency light emitting devices in silicon," *Mater. Sci. Eng. B*, vol. 83, p. 105, 2003.

[32] S. McNab, N. Moll, and Y. Vlasov, "Ultra-low loss photonic integrated circuit with membrane-type photonic crystal waveguides," *Opt. Express*, vol. 11, pp. 2927–2939, 2003.

[33] Y. A. Vlasov and S. J. McNab, "Losses in single-mode silicon-on-insulator strip waveguides and bends," *Opt. Express*, vol. 12, pp. 1622–1631, 2004.

[34] S. J. Koester, J. D. Schaub, G. Dehlinger, J. O. Chu, Q. C. Ouyang, and A. Grill, "High-efficiency, Ge-on-SOI lateral PIN photodiodes with 29 GHz bandwidth," in *Proc. Device Res. Conf.*, 2004.

[35] A. Liu, R. Jones, L. Liao, D. Samara Rubio, D. Rubin, O. Cohen, R. Nicolaescu, and M. Paniccia, "A high-speed silicon optical modulator based on a metal-oxide-semiconductor capacitor," *Nature*, vol. 427, pp. 615–618, 2004.

[36] V. Raghunathan, R. Claps, D. Dimitropoulos, and B. Jalali, "Wavelength conversion in silicon using Raman induced four-wave mixing," *Appl. Phys. Lett.*, vol. 85, pp. 34–36, 2004.

[37] V. R. Almeida, C. A. Barrios, R. R. Panepucci, and M. Lipson, "All optical control of light on a silicon chip," *Nature*, vol. 431, pp. 1081–1084, 2004.

[38] O. Boyraz, P. Koonath, V. Raghunathan, and B. Jalali, "All optical switching and continuum generation in silicon waveguides," *Opt. Express*, vol. 12, pp. 4094–4102, 2004.

[39] H. Rong, A. Liu, R. Jones, O. Cohen, D. Hak, R. Nicolasecu, A. Fang, and M. Paniccia, "An all-silicon Raman laser," *Nature*, vol. 435, pp. 292–294, 2005.

[40] L. Liao, D. Samara-Rubio, M. Morse, A. Liu, D. Hodge, D. Rubin, U. D. Keil, and T. Franck, "High speed silicon Mach-Zehnder," *Opt. Express*, vol. 13, pp. 3129–3135, 2005.

[41] C. Gunn, "CMOS photonics for high-speed interconnects," *IEEE Micro*, vol. 26, pp. 58–66, 2006.

[42] A. W. Fang, H. Park, O. Cohen, R. Jones, M. Paniccia, and J. Bowers, "Electrically pumped hybrid AlGaInAs-silicon evanescent laser," *Opt. Express*, vol. 14, pp. 9203–9210, 2006.

[43] M. A. Foster, A. C. Turner, J. E. Sharping, B. S. Schmidt, M. Lipson, and A. L. Gaeta, "Broadband optical parametric gain on a silicon photonic chip," *Nature*, vol. 441, pp. 960–963, 2006.

[44] J. Fage-Pedersen, L. A. Frandsen, A. Lavrinenko, and P. I. Borel, "A linear electrooptic effect in silicon, induced by use of strain," in *Part of: 2006 EEE/LEOS Int. Conf. on Proc. 3rd Group IV Photon.*, 2006, pp. 37–39.

[45] F. Xia, L. Sekaric, M. O'Boyle, and Y. Vlasov, "Coupled resonator optical waveguides based on silicon-on-insulator photonic wires," *Appl. Phys. Lett.*, vol. 89, p. 041122, 2006.

[46] Van Campenhout, P. R. Romeo, P. Regreny, C. Seassal, D. Van Thourhout, S. Verstuyft, L. Di Cioccio, J.-M. Fedeli, C. Lagahe, and R. Baets, "Electrically pumped InP-based microdisk lasers integrated with a nanophotonic silicon-on-insulator waveguide circuit," *Opt. Express*, vol. 15, pp. 6744–6749, 2007.

[47] B. R. Koch, A. W. Fang, O. Cohen, and J. E. Bowers, "Mode-locked silicon evanescent lasers," *Opt. Express*, vol. 15, pp. 11 225–11 233, 2007.

[48] T. Yin, R. Cohen, M. Morse, G. Sarid, Y. Chetrit, D. Rubin, and M. J. Paniccia, "31 GHz Ge n-i-p waveguide photodetectors on silicon-on-insulator substrate," *Opt. Express*, vol. 15, pp. 13 965–13 971, 2007.

[49] A. Liu, L. Liao, D. Rubin, J. Basak, H. Nguyen, Y. Chetrit, R. Cohen, N. Izhaky, and M. Paniccia, "Silicon optical modulator for high-speed applications," in *Proc. 4th IEEE Int. Conf. Group IV Photon.*, 2007, pp. 1–3.

[50] G. Masini, G. Capellini, J. Witzens, and C. Gunn, "A four-channel, 10 Gbps monolithic optical receiver in 130 nm CMOS with integrated Ge waveguide photodetectors," presented at the National Fiber Optic Engineers Conf., 2007, Paper PDP31, unpublished.

[51] F. Xia, L. Sekaric, and Y. Vlasov, "Ultracompact optical buffers on a silicon chip," *Nat. Photon.*, vol. 1, pp. 65–71, 2007.

[52] Y. Vlasov, W. M. J. Green, and F. Xia, "High-throughput silicon nanophotonic deflection switch for on-chip optical networks," *Nat. Photon.*, vol. 2, pp. 242–246, 2008.

[53] S. Ossicini, L. Pavesi, and F. Priolo, "Light emitting silicon for microphotonics," in *Springer Tracts in Modern Physics*, vol. 194. Berlin, Germany: Springer-Verlag, 2003.

[54] P. M. Fauchet, "Light emission from Si quantum dots," *Mater. Today*, vol. 8, pp. 23–26, 2005.

[55] L. Pavesi, "Routes towards silicon-based lasers," *Mater. Today*, vol. 8, pp. 23–26, 2005.

[56] G. Qin and Y. Jia, "Mechanism of visible luminescence in porous silicon," *Solid State Commun.*, vol. 86, pp. 559–563, 1993.

[57] O. Bisi, S. Ossicini, and L. Pavesi, "Porous silicon: A quantum sponge structure for silicon based optoelectronics," *Surf. Sci. Rep.*, vol. 38, pp. 1–126, 2000.

[58] S. G. Cloutier, P. A. Kossyrev, and J. Xu, "Optical gain and stimulated emission in periodic nanopatterned crystalline silicon," *Nat. Mater.*, vol. 4, pp. 887–891, 2005.

[59] M. A. Green, J. Zhao, A. Wang, P. J. Reece, and M. Gal, "Efficient silicon light-emitting diodes," *Nature*, vol. 412, pp. 805–808, 2001.

[60] W. L. Ng, M. A. Lourenço, R. M. Gwilliam, S. Ledain, G. Shao, and K. P. Homewood, "An efficient room-temperature silicon-based light-emitting diode," *Nature*, vol. 410, pp. 192–194, 2001.

[61] A. M. Emel'yanov, N. A. Sobolev, and E. I. Shek, "Silicon LEDs emitting in the band-to-band transition region: Effect of temperature and current strength," *Phys. Solid State*, vol. 46, pp. 40–44, 2004.

[62] M. Kittler, T. Arguirov, A. Fischer, and W. Seifert, "Silicon-based light emission after ion implantation," *Opt. Mater.*, vol. 27, pp. 967–972, 2005.

[63] Z. Yuan, D. Li, D. Gong, M. Wang, R. Fan, and D. Yang, "Effects of defect, carrier concentration and annealing process on the photoluminescence of silicon pn diodes," *Mater. Sci. Semi. Process.*, vol. 10, pp. 173–178, 2007.

[64] J. Liu, X. Sun, D. Pan, X. Wang, L. C. Kimerling, T. L. Koch, and J. Michel, "Tensile-strained, n-type Ge as a gain medium for monolithic laser integration on Si," *Opt. Express*, vol. 15, p. 11272, 2007.

[65] E. O. Sveinbjornsson and J. Wdber, "Room temperature electroluminescence from dislocation-rich silicon," *Appl. Phys. Lett.*, vol. 69, pp. 2686–2688, 1996.

[66] V. V. Kveder, M. Badylevich, E. A. Steinman, and A. Lzotov, "Room-temperature silicon light-emitting diodes based on dislocation luminescence," *Appl. Phys. Lett.*, vol. 84, pp. 2106–2108, 2004.

[67] D. Leong, M. Harry, K. J. Reeson, and K. P. Homewood, "A silicon/iron-disilicide light-emitting diode operating at a wavelength of 1.5 μm," *Nature*, vol. 387, pp. 686–688, 1997.

[68] C. Li, T. Suemasu, and F. Hasegawa, "Room-temperature electroluminescence of a Si-based p-i-n diode with β–$FeSi_2$ particles embedded in the intrinsic silicon," *J. Appl. Phys.*, vol. 97, p. 043529, 2005.

[69] H. Rong, R. Jones, A. Liu, O. Cohen, D. Hak, A. Fang, and M. Paniccia, "A continuous-wave Raman silicon laser," *Nature*, vol. 434, pp. 1–3, 2005.

[70] N. Daldosso, D. Navarro-Urrios, M. Melchiorri, C. Garcia, P. Pellegrino, B. Garrido, C. Sada, G. Battaglin, F. Gourbilleau, R. Rizk, and L. Pavesi, "Er coupled Si nanocluster waveguide," *IEEE J. Sel. Topics Quantum Electron.*, vol. 12, pp. 1607–1617, 2006.

[71] J. Sun, W. Skorupa, T. Dekorsy, and M. Helm, "Efficient ultraviolet electroluminescence from a Gd-implanted silicon metal-oxide-semiconductor device," *Appl. Phys. Lett.*, vol. 85, pp. 3387–3389, 2004.

[72] Z. Yuan, D. Li, M. Wang, P. Chen, D. Gong, L. Wang, and D. Yang, "Photoluminescence of Tb^{3+} doped SiN_x films grown by plasma-enhanced chemical vapor deposition," *J. Appl. Phys.*, vol. 100, p. 083106, 2006.

[73] W. Skorupa, J. Sun, S. Prucnal, L. Rebohle, T. Gebel, A. N. Nazarov, I. N. Osiyuk, and M. Helm, "Rare earth ion implantation for silicon based light emission," *Solid State Phenom.*, vol. 108–109, pp. 755–760, 2005.

[74] R. D. Tilley, J. H. Warner, K. Yamamoto, I. Matsui, and H. Fujimori, "Micro-emulsion synthesis of monodisperse surface stabilized silicon nanocrystals," *Chem. Commun.*, vol. 14, pp. 1833–1835, 2005.

[75] L. Wang, Z. Ma, X. Huang, Z. Li, J. Li, Y. Bao, J. Xu, W. Li, and K. Chen, "The room-temperature visible photoluminescence from nanocrystalline Si in Si/SiN_x superlattices," *Solid State Commun.*, vol. 117, pp. 239–244, 2001.

[76] N. M. Park, C. J. Choi, T. Y. Seong, and S. J. Park, "Quantum confinement in amorphous silicon quantum dots embedded in silicon nitride," *Phys. Rev. Lett.*, vol. 86, pp. 1355–1357, 2001.

[77] M. Wang, D. Li, Z. Yuan, D. Yang, and D. Que, "Photoluminescence of Si-rich silicon nitride: Defect-related states and silicon nanoclusters," *Appl. Phys. Lett.*, vol. 90, p. 131903, 2007.

[78] D. Y. Song, E. C. Cho, G. Conibeer, C. Flynn, Y. D. Huang, and M. A. Green, "Structural, electrical and photovoltaic characterization of Si nanocrystals embedded SiC matrix and Si nanocrystals/c-Si heterojunction devices," *Solar Energy Mater. Solar Cells*, vol. 92, pp. 474–481, 2008.

[79] M. S. Hybertsen, "Absorption and emission of light in nanoscale silicon structures," *Phys. Rev. Lett.*, vol. 72, pp. 1514–1517, 1994.

[80] M. Zacharias, J. Heitmann, R. Scholz, U. Kahler, M. Schmidt, and J. Blasing, "Size-controlled highly luminescent silicon nanocrystals: A SiO/SiO_2 superlattice approach," *Appl. Phys. Lett.*, vol. 80, pp. 661–663, 2002.

[81] J. Valenta, R. Juhasz, and J. Linnros, "Photoluminescence spectroscopy of single silicon quantum dots," *Appl. Phys. Lett.*, vol. 80, pp. 1070–1072, 2002.

[82] V. Kumar, *Nanosilicon*. Oxford, UK: Elsevier, 2007.

[83] B. Averboukh, R. Huber, K. W. Cheah, Y. Shen, G. Qin, Z. Ma, and W. Zong, "Luminescence studies of a Si/SiO_2 superlattice," *J. Appl. Phys.*, vol. 92, pp. 3564–3568, 2002.

[84] G. Hadjisavvas and P. C. Kelires, "Structure and energetics of Si nanocrystals embedded in a-SiO_2," *Phys. Rev. Lett.*, vol. 93, p. 226104, 2004.

[85] X. Wang, J. Zhang, L. Ding, B. Cheng, W. Ge, J. Yu, and Q. Wang, "Origin and evolution of photoluminescence from Si nanocrystals embedded in a SiO_2 matrix," *Phys. Rev. B*, vol. 72, p. 195313, 2005.

[86] M. Luppi and S. Ossicini, "Multiple Si = O bonds at the silicon cluster surface," *J. Appl. Phys.*, vol. 94, pp. 2130–2132, 2003.

[87] M. V. Wolkin, J. Jorne, P. M. Fauchet, G. Allan, and C. Delerue, "Electronic states and luminescence in porous silicon quantum dots: The role of oxygen," *Phys. Rev. Lett.*, vol. 82, pp. 197–200, 1999.

[88] N. Daldosso, M. Luppi, S. Ossicini, E. Degoli, R. Magri, G. Dalba, P. Fornasini, R. Grisenti, F. Rocca, L. Pavesi, S. Boninelli, F. Priolo, C. Bongiorno, and F. Iacona, "Role of the interface region on the optoelectronic properties of silicon nanocrystals embedded in SiO_2," *Phys. Rev. B*, vol. 68, p. 085327, 2003.

[89] E. Lioudakis, A. Antoniou, A. Othonos, C. Christofides, A. G. Nassiopoulou, C. B. Lioutas, and N. Frangis, "The role of surface vibrations and quantum confinement effect to the optical properties of very thin nanocrystalline silicon films," *J. Appl. Phys.*, vol. 102, p. 083534, 2007.

[90] S. Godefroo, M. Hayne, M. Jivanescu, A. Stesmans, M. Zacharias, O. I. Lebedev, G. V. Tendeloo, and V. V. Moshchalkov, "Classification and control of the origin of photoluminescence from Si nanocrystals," *Nat. Nanotech.*, vol. 3, pp. 174–178, 2008.

[91] J. Robertson and M. J. Powell, "Gap states in silicon nitride," *Appl. Phys. Lett.*, vol. 44, pp. 415–417, 1984.

[92] M. Wang, M. Xie, L. Ferraioli, Z. Yuan, D. Li, D. Yang, and L. Pavesi, "Light emission properties and mechanism of low-temperature prepared amorphous SiNx films. I. Room-temperature band tail states photoluminescence," *J. Appl. Phys.*, vol. 104, p. 083504, 2008.

[93] A. Irrera, D. Pacifici, M. Miritello, G. Franzo, F. Priolo, F. Iacona, D. Sanfilippo, G. Di Stefano, and P. G. Fallica, "Electroluminescence properties of light emitting devices based on silicon nanocrystals," *Phys. E*, vol. 16, pp. 395–399, 2003.

[94] J. Valenta, N. Lalic, and J. Linros, "Electroluminescence of single silicon nanocrystals," *Appl. Phys. Lett.*, vol. 84, pp. 1459–1461, 2004.

[95] P. Photopoulos and A. G. Nassiopoulou, "Room-and low-temperature voltage tunable electroluminescence from a single layer of silicon quantum dots in between two thin SiO_2 layers," *Appl. Phys. Lett.*, vol. 77, pp. 1816–1818, 2000.

[96] N. Lalic and J. Linnros, "Light emitting diode structure based on Si nanocrystals formed by implantation into thermal oxide," *J. Lumin.*, vol. 80, pp. 263–267, 1999.

[97] N.-M. Park, T.-S. Kim, and S.-J. Park, "Band gap engineering of amorphous silicon quantum dots for light-emitting diodes," *Appl. Phys. Lett.*, vol. 78, pp. 2575–2577, 2001.

[98] M. Peralvarez, C. Garcìa, M. Lopez, B. Garrido, J. Barreto, C. Dominguez, and J. A. Rodriguez, "Field effect luminescence from Si nanocrystals obtained by plasma-enhanced chemical vapor deposition," *Appl. Phys. Lett.*, vol. 89, p. 051112, 2006.

[99] M. Wang, A. Anopchenko, A. Marconi, E. Moser, S. Prezioso, L. Pavesi, G. Pucker, P. Bellutti, and L. Vanzetti, "Light emitting devices based on nanocrystalline-silicon multilayer structure," *Phys. E*, vol. 41, pp. 912–915, 2009.

[100] S. Prezioso, A. Anopchenko, Z. Gaburro, L. Pavesi, G. Pucker, L. Vanzetti, and P. Bellutti, "Electrical conduction and electroluminescence in nanocrystalline silicon-based light emitting devices," *J. Appl. Phys.*, vol. 104, p. 063103, 2008.

[101] B. De Salvo, G. Ghibaudo, P. Luthereau, T. Baron, B. Guillaumot, and G. Reimbold, "Transport mechanisms and charge trapping in thin dielectric/Si nano-crystals structures," *Solid-State Electron.*, vol. 45, pp. 1513–1519, 2001.

[102] J. Maserjian, "Tunneling in thin MOS structures," *J. Vac. Sci. Technol.*, vol. 11, pp. 996–1003, 1974.

[103] S. M. Hossain, A. Anopchenko, S. Prezioso, L. Ferraioli, L. Pavesi, G. Pucker, P. Bellutti, S. Binetti, and M. Acciarri, "Sub-band gap photo-response of nano-crystalline silicon in a metal-oxide-semiconductor device," *J. Appl. Phys.*, vol. 104, p. 074917, 2008.

[104] D. J. DiMaria, J. R. Kirtley, E. J. Pakulis, D. W. Dong, T. S. Kuan, F. L. Pesavento, T. N. Theis, J. A. Cutro, and S. D. Brorson, "Electroluminescence studies in silicon dioxide films containing tiny silicon islands," *J. Appl. Phys.*, vol. 56, pp. 401–415, 1984.

[105] G. Conibeer, M. A. Green, R. Corkish, Y. Cho, E. C. Cho, C. Jiang, T. Fangsuwannarak, E. Pink, Y. Huang, T. Puzzer, T. Trupke, B. Richards, A. Shalav, and K. Lin, "Silicon nanostructures for third generation photovoltaic solar cells," *Thin Solid Films*, vol. 511–512, pp. 654–662, 2006.

[106] J. Cai and C. T. Sah, "Gate tunneling currents in ultrathin oxide metal-oxide-silicon transistors," *J. Appl. Phys.* vol. 89, pp. 2272–2285, 2001.

[107] B. Garrido, C. Garcìa, S.-Y. Seo, P. Pellegrino, D. Navarro-Urrios, N. Daldosso, L. Pavesi, F. Gourbilleau, and R. Rizk, "Excitable Er fraction and quenching phenomena in Er-doped SiO_2 layers containing Si nanoclusters," *Phys. Rev. B*, vol. 76, p. 245308, 2007.

[108] L. Dal Negro, M. Cazzanelli, N. Daldosso, Z. Gaburro, L. Pavesi, F. Priolo, D. Pacifici, G. Franzò, and F. Iacona, "Stimulated emission in plasma enhanced chemical vapour deposited silicon nanocrystals," *Phys. E*, vol. 16, pp. 297–308, 2003.

[109] A. Polman and F. C. J. M. van Veggel, "Broadband sensitizers for erbium-doped planar optical amplifiers: Review," *J. Opt. Soc. Amer. B*, vol. 21, pp. 871–892, 2004.

[110] F. Priolo, G. Franzò, D. Pacifici, V. Vinciguerra, F. Iacona, and A. Irrera, "Role of the energy transfer in the optical properties of undoped and Er-doped interacting Si nanocrystals," *J. Appl. Phys.*, vol. 89, pp. 264–272, 2001.

[111] A. J. Kenyon, C. E. Chryssou, C. W. Pitt, T. Shimizu-Iwayama, D. E. Hole, N. Sharma, and C. J. Humphreys, "Luminescence from erbium-doped silicon nanocrystals in silica: Excitation mechanisms," *J. Appl. Phys.*, vol. 91, pp. 367–374, 2002.

[112] P. G. Kik and A. Polman, *Towards the First Silicon Laser*, ser. NATO Science II, L. Pavesi *et al.*, Eds. Dordrecht, The Netherlands: Kluwer, 2003, 2003.

[113] D. Pacifici, G. Franzò, F. Priolo, F. Iacona, and L. Dal Negro, "Modeling and perspectives of the Si nanocrystals-Er interaction for optical amplification," *Phys. Rev. B*, vol. 67, p. 245301, 2003.

[114] C. J. Oton, W. H. Loh, and A. J. Kenyon, "Er^{3+} excited state absorption and the low fraction of nanocluster-excitable Er^{3+} in SiO_x," *Appl. Phys. Lett.*, vol. 89, p. 031116, 2006.

[115] I. Izeddin, T. Gregorkiewicz, and M. Fujii, "Non-radiative sub-microsecond recombination of excited Er^{3+} ions in SiO_2 sensitized with Si nanocrystals," *Phys. E*, vol. 38, pp. 144–147, 2007.

[116] D. Navarro-Urrios, N. Daldosso, C. Garcìa, P. Pellegrino, B. Garrido, F. Gourbilleau, R. Rizk, and L. Pavesi, "Signal enhancement and limiting factors in waveguides containing Si nanoclusters and Er^{3+} ions," *Jpn. J. Appl. Phys.*, vol. 46, pp. 6626–6633, 2007.

[117] A. Pitanti, D. Navarro-Urrios, R. Guider, N. Daldosso, F. Gourbilleau, L. Khomenkova, R. Rizk, and L. Pavesi, "Further improvements in Er^{3+} coupled to Si nanoclusters rib waveguides," in *Proc. SPIE*, 2008, vol. 6996, p. 699619.

[118] M. Wojdak, M. Klik, M. Forcales, O. B. Gusev, T. Gregorkiewicz, D. Pacifici, G. Franzò, F. Priolo, and F. Iacona, "Sensitization of Er luminescence by Si nanoclusters," *Phys. Rev. B*, vol. 69, p. 233315, 2004.

[119] J. Lee, J. H. Shin, and N. Park, "Optical Gain at 1.5 μm in nanocrystal Si-sensitized Er-doped silica waveguide using top-pumping 470 nm LEDs," *J. Lightw. Technol.*, vol. 23, pp. 19–25, 2005.

[120] F. Gourbilleau, M. Levalois, C. Dufour, J. Vicens, and R. Rizk, "Optimized conditions for an enhanced coupling rate between Er ions and Si nanoclusters for an improved 1.54-μm emission," *J. Appl. Phys.*, vol. 95, pp. 3717–3722, 2004.

[121] Z. Gaburro, P. Bettotti, N. Daldosso, M. Ghulinyan, D. Navarro-Urrios, M. Melchiorri, F. Riboli, M. Saiani, F. Sbrana, and L. Pavesi, "Nanostructured silicon for photonics-from materials to devices," in *Material Science Foundations*, vol. 27–28. Zurich, Switzerland: Trans Tech, 2006.

[122] D. Navarro-Urrios, F. Riboli, M. Cazzanelli, N. Daldosso, L. Pavesi, C. J. Oton, J. Heitmann, L. X. Yi, R. Scholz, and M. Zacharias, "Birefringence characterization of mono-dispersed Silicon nanocrystals planar waveguides," *Opt. Mater.*, vol. 27, pp. 763–768, 2005.

[123] J. Ruan, P. M. Fauchet, L. Dal Negro, M. Cazzanelli, and L. Pavesi, "Stimulated emission in nanocrystalline silicon superlattices," *J. Appl. Phys.*, vol. 83, pp. 5479–5481, 2003.

[124] L. Dal Negro, M. Cazzanelli, B. Danese, L. Pavesi, F. Iacona, G. Franzò, and F. Priolo, "Light amplification in silicon nanocrystals by pump and probe transmission measurements," *J. Appl. Phys.*, vol. 96, pp. 5747–5755, 2004.

[125] L. Khriachtchev, M. Räsänen, and S. Novikov, "Efficient wavelength-selective optical waveguiding in a silica layer containing Si nanocrystals," *Appl. Phys. Lett.*, vol. 83, pp. 3018–3020, 2003.

[126] N. Daldosso, M. Melchiorri, L. Pavesi, G. Pucker, F. Gourbilleau, S. Chausserie, A. Belarouci, X. Portier, and C. Dufour, "Optical losses and absorption cross section of silicon nanocrystals," *J. Lumin.*, vol. 121, pp. 344–348, 2006.

[127] W. Spitzer and H. Y. Fan, "Infrared absorption in n-type silicon," *Phys. Rev.*, vol. 108, pp. 268–271, 1957.

[128] R. G. Elliman, M. J. Lederer, N. Smith, and B. Luther-Davies, "The fabrication and properties of silicon-nanocrystal-based devices and structures produced by ion implantation—The search for gain," *Nucl. Instrum. Methods B*, vol. 206, pp. 427–431, 2003.

[129] R. G. Elliman, M. Forcales, A. R. Wilkinson, and N. J. Smith, "Waveguiding properties of Er-implanted silicon-rich oxides," *Nucl. Instrum. Methods B*, vol. 257, pp. 11–14, 2007.

[130] D. Navarro-Urrios, A. Pitanti, N. Daldosso, F. Gorbilleau, R. Rizk, G. Pucker, and L. Pavesi, "Quantification of the carrier absorption losses in Si-nanocrystal rich rib waveguides at 1.54 μm," *Appl. Phys. Lett.*, vol. 92, p. 051101, 2008.

[131] E. Jordana, J.-M. Fedeli, J.-M. Fedeli, P. Lyan, J. P. Colonna, P. Gautier, N. Daldosso, L. Pavesi, Y. Lebour, P. Pellegrino, B. Garrido, J. Blasco, F. Cuesta-Soto, and P. Sanchis, "Deep-UV lithography fabrication of slot waveguides and sandwiched waveguides for nonlinear applications," in *Proc. 4th IEEE Int. Conf. Group IV Photon.*, 2007, pp. 217–219.

[132] D. S. Gardner and M. L. Brongersma, "Microring and microdisk optical resonators using silicon nanocrystals and erbium prepared using silicon technology," *Opt. Mater.*, vol. 27, pp. 804–811, 2005.

[133] A. Polman, B. Min, J. Kalkman, T. J. Kippenberg, and K. J. Vahala, "Ultralow-threshold erbium-implanted toroidal microlaser on silicon," *Appl. Phys. Lett.*, vol. 84, pp. 1037–1039, 2004.

[134] M. Lipson, "Guiding, modulating, and emitting light on silicon—Challenges and opportunities," *J. Lightw. Technol.*, vol. 23, pp. 4222–4238, 2005.

[135] Y. Lebour, R. Guider, E. Jordana, J.-M. Fedeli, P. Pelligrino, S. Hernández, B. Garrido, N. Daldosso, and L. Pavesi, "High coupled ring resonators based on silicon clusters slot waveguide," in *Proc. 5th IEEE Int. Conf. Group IV Photon.*, 2008.

[136] A. Yariv, Y. Xu, R. K. Lee, and A. Scherer, "Coupled-resonator optical waveguide: A proposal and analysis," *Opt. Lett.*, vol. 24, pp. 711–713, 1999.

[137] L. Thévenaz, "Slow and fast light in optical fibres," *Nat. Photon.*, vol. 2, pp. 474–481, 2008.

[138] T. Baba, "Slow light in photonic crystals," *Nat. Photon.*, vol. 2, pp. 465–473, 2008.

[139] F. Xia, L. Sekaric, and Y. Vlasov, "Ultracompact optical buffers on a silicon chip," *Nat. Photon.*, vol. 1, pp. 65–71, 2006.

[140] A. Di Falco, L. O'Faolain, and T. F. Krauss, "Dispersion control and slow light in slotted photonic crystal waveguides," *Appl. Phys. Lett.*, vol. 92, p. 083501, 2008.

[141] F. Riboli, P. Bettotti, and L. Pavesi, "Band gap characterization and slow light effects in one dimensional photonic crystals based on silicon slot-waveguides," *Opt. Express*, vol. 15, pp. 11 769–11 775, 2007.

[142] A. Pitanti, P. Bettotti, E. Rigo, R. Guider, N. Daldosso, J.-M. Fedeli, and L. Pavesi, "Coupled cavities in one-dimensional photonic crystal based on horizontal slot waveguide structure with Si-nc," in *Proc. 5th IEEE Int. Conf. Group IV Photon.*, 2008.

[143] L. Rayleigh, "Further applications of Bessel's functions of high order to the whispering gallery and allied problems," *Phil. Mag.*, vol. 27, pp. 100–104, 1914.

[144] Z. Zhang, L. Yang, V. Liu, T. Hong, K. Vahala, and A. Scherer, "Visible submicron microdisk lasers," *Appl. Phys. Lett.*, vol. 90, p. 111119, 2007.

[145] K. Srinivasan, A. Stintz, S. Krishna, and O. Painter, "Photoluminescence measurements of quantum-dot-containing semiconductor microdisk resonators using optical fiber taper waveguides," *Phys. Rev. B*, vol. 72, p. 205318, 2005.

[146] P. Del'Haye, O. Arcizet, A. Schliesser, R. Holzwarth, and T. J. Kippenberg, "Full stabilization of a microresonator frequency comb," *Phys. Rev. Lett.*, vol. 101, p. 053903, 2008.

[147] A. Schliesser, G. Anetsberger, R. Rivière, O. Arcizet, and T. J. Kippenberg, "High-sensitivity monitoring of micromechanical vibration using optical whispering gallery mode resonators," *New J. Phys.*, vol. 10, p. 095015, 2008.

[148] A. M. Armani and K. J. Vahala, "Heavy water detection using ultra-high-Q microcavities," *Opt. Lett.*, vol. 31, pp. 1896–1898, 2006.

[149] T. Aoki, "Observation of strong coupling between one atom and a monolithic microresonator," *Nature*, vol. 443, pp. 671–674, 2006.

[150] R. J. Zhang, S. Y. Seo, A. P. Milenin, M. Zacharias, and U. Gösele, "Visible range whispering-gallery mode in microdisk array based on size-controlled Si nanocrystals," *Appl. Phys. Lett.*, vol. 88, p. 153120, 2006.

[151] M. Ghulinyan, D. Navarro-Urrios, A. Pitanti, A. Lui, G. Pucker, and L. Pavesi, "Whispering-gallery modes and light emission from a Si-nanocrystal-based single microdisk resonator," *Opt. Express*, vol. 16, pp. 13 218–13 224, 2008.

[152] A. J. Nozik, "Quantum dot solar cells," *Phys. E*, vol. 14, pp. 115–120, 2002.

[153] M. A. Green, "Third generation photovoltaics: Solar cells for 2020 and beyond," *Phys. E*, vol. 14, pp. 65–70, 2002.

[154] W. Schockley and H. J. Queisser, "Detailed balance limit of efficiency of p-n junction solar cells," *J. Appl. Phys.*, vol. 32, pp. 510–519, 1961.

[155] E. C. Cho, Y. H. Cho, T. Trupke, R. Corkish, G. Conibeer, and M. A. Green, in *Proc. 19th Eur. Photovoltaic Solar Energy Conf.*, Paris, France, 2004, pp. 235–238.

[156] C. Jiang, E. C. Cho, G. Conibeer, and M. A. Green, in *Proc. 19th Eur. Photovoltaic Solar Energy Conf.*, Paris, France, 2004, pp. 80–83.

[157] C. Jiang and M. A. Green, "Silicon quantum dot superlattices: Modeling of energy bands, densities of states, and mobilities for silicon tandem solar cell applications," *J. Appl. Phys.*, vol. 99, p. 114902, 2006.

[158] E. C. Cho, M. A. Green, G. Conibeer, D. Y. Song, Y. H. Cho, G. Scardera, S. J. Huang, S. Park, X. J. Hao, Y. Huang, and L. V. Dao, "Silicon quantum dots in a dielectric matrix for all-silicon tandem solar cells," *Adv. Opto. Electr.*, vol. 2007, 2007.

[159] R. Rolver, B. Berghoff, D. L. Batzner, B. Spangenberg, and H. Kurz, "Lateral Si/SiO_2 quantum well solar cells," *Appl. Phys. Lett.*, vol. 92, p. 212108, 2008.

[160] R. Rolver, B. Berghoff, D. Batzner, B. Spangenberg, H. Kurz, M. Schmidt, and B. Stegemann, " Si/SiO_2 multiple quantum wells for all silicon tantem cells: Conductivity and photocurrent measurements," *Thin Solid Films*, vol. 516, pp. 6763–6766, 2008.

[161] T. Arguirov, T. Mchedlidze, M. Kittler, R. Rolver, B. Berghoff, M. Forst, and B. Spangenberg, "Residual stress in Si nanocrystals embedded in a SiO_2 matrix," *Appl. Phys. Lett.*, vol. 89, p. 053111, 2006.

[162] T. Mchedlidze, T. Arguirov, S. Kouteva-Arguirova, G. Jia, M. Kittler, R. Rolver, B. Berghoff, M. Forst, D. L. Batzner, and B. Spangenberg, "Influence of a substrate, structure and annealing procedures on crystalline and optical properties of Si/SiO_2 multiple quantum wells," *Thin Solid Films*, vol. 516, pp. 6800–6803, 2008.

[163] P. T. Landsberg, H. Nussbaumer, and G. Willeke, "Band-band impact ionization and solar cell efficiency," *J. Appl. Phys.*, vol. 74, pp. 1451–1452, 1993.

[164] S. Kolodinski, J. H. Werner, T. Wittchen, and H. J. Queisser, "Quantum efficiencies exceeding unity due to impact ionization in silicon solar cells," *Appl. Phys. Lett.*, vol. 63, pp. 2405–2407, 1993.

[165] M. C. Beard, K. P. Knutsen, P. Yu, J. M. Luther, Q. Song, W. K. Metzger, R. J. Ellingson, and A. J. Nozik, "Multiple exciton generation in colloidal silicon nanocrystals," *Nano Lett.*, vol. 7, pp. 2506–2512, 2007.

[166] L. E. Ramos, E. Degoli, G. Cantele, S. Ossicini, D. Ninno, J. Furthmuller, and F. Bechstedt, "Structural features and electronic properties of group-III-, group-IV-, and group-V-doped Si nanocrystallites," *J. Phys.: Condens. Matter*, vol. 19, p. 466211, 2007.

[167] R. Spano, N. Daldosso, M. Cazzanelli, L. Ferraioli, L. Tartara, J. Yu, V. Degiorgio, E. Jordana, J. M. Fedeli, and L. Pavesi, "Bound electronic and free carrier nonlinearities in Silicon nanocrystals at 1550 nm," *Opt. Express*, vol. 17, pp. 3941–3950, 2009.

[168] R. L. Sutherland, *Handbook of Nonlinear Optics*. New York: Marcel Dekker, 2003.

[169] R. Adair, L. L. Chase, and S. A. Payne, "Nonlinear refractive index of optical crystals," *Phys. Rev. B*, vol. 39, pp. 3337–3350, 1989.

[170] M. Dinu, F. Quochi, and H. Garcia, "Third-order nonlinearities in silicon at telecom wavelengths," *Appl. Phys. Lett.*, vol. 82, pp. 2954–2956, 2003.

[171] M. Sheik-Bahae, A. A. Said, T.-H. Wei, D. A. Hagan, and E. W. Van Stryland, "Sensitive measurements of optical nonlinearities using a single beam," *IEEE J. Quantum Electron.*, vol. 26, pp. 760–769, 1990.

[172] G. V. Prakash, M. Cazzanelli, Z. Gaburro, L. Pavesi, F. Iacona, G. Franzò, and F. Priolo, "Linear and nonlinear optical properties of plasma enhanced chemical-vapour deposition grown Silicon nanocrystals," *J. Modern Opt.*, vol. 49, pp. 719–730, 2002.

[173] S. Hernández, P. Pellegrino, A. Martínez, Y. Lebour, B. Garrido, R. Spano, M. Cazzanelli, N. Daldosso, L. Pavesi, E. Jordana, and J. M. Fedeli, "Linear and non-linear optical properties of Si nanocrystals in SiO_2 deposited by PECVD," *J. Appl. Phys.*, vol. 103, p. 064309, 2008.

ABOUT THE AUTHORS

Zhizhong Yuan was born in Shijia Zhuang, Hebei, China, in 1977. He graduated from the School of Materials Science and Engineering, Jiangsu University, China, in 2000. He received the Dr.Eng. degree in materials science and engineering from State Key Laboratory of Silicon Materials, Zhejiang University, China, in 2007.

He is a Postdoctoral Researcher with the Nanoscience Laboratory, Department of Physics, University of Trento, Italy. His research interests include silicon-based light emitting materials and devices and advanced solar cells.

Aleksei Anopchenko graduated from Kharkov Polytechnic Institute, Ukraine, in 1993. He received the Ph.D. degree in solid-state physics from Comenius University, Bratislava, Slovakia, in 2001.

He was an Engineer with the B. I. Verkin Institute for Low Temperature Physics and Engineering, National Academy of Sciences of Ukraine, in 1993–1997 and a Research Associate with the Institute of Physics, Slovak Academy of Sciences, in 1997–2001. From 2001 to 2004, he was a Guest Researcher with the Polymers Division, NIST, Gaithersburg, MD. Since 2007, he has been a Research Fellow with the Nanoscience Laboratory, Department of Physics, University of Trento, Italy, working on an Intel-funded and several European research projects. His research interests include silicon micro- and nanophotonic devices, light-emitting devices, photovoltaics, polymer composite materials, dielectric relaxation and impedance spectroscopy, and microwave and x-ray scattering techniques.

Nicola Daldosso was born in Verona, Italy, 1972. He graduated in physics from the University of Trento, Italy, in 1997. He received the Ph.D. degree in physics of matter from the Université J. Fourier, Grenoble, France, in 2001.

From 1998 to 2000, he was with the Italian beamline GILDA, European Synchrotron Radiation Facilities, Grenoble. In 2001, he joined the Nanoscience Laboratory, Department of Physics, University of Trento, as a Senior Associate Researcher. His research interests include structural and optical properties of nanostructures materials, in particular silicon nanocrystals as well as erbium-doped ones, and, more recently, integrated optoelectronics on silicon. He is involved in several EU research projects on Si-based photonics. He is the author of about 70 papers, coauthor of five books, and has received one patent. He has been an invited participant to 12 international conferences and is the referee of several international scientific journals. He holds an H-number of 11.

Romain Guider was born in Verdun, France, 1983. He graduated in optoelectronics engineering from Ecole Nationale Supérieure des Sciences Appliquées et de Technologie, France, in 2006. He is currently pursuing the Ph.D. degree from the Nanoscience Laboratory, Department of Physics, University of Trento, Italy.

His research interests include silicon-based waveguides and photonics building blocks like ring resonators and optical properties of silicon-based polymer derived ceramics.

Daniel Navarro-Urrios was born in Santa Cruz de Tenerife, Spain, on October 23, 1978. He graduated in physics and received the Ph.D. degree from the University of La Laguna, Spain, in 2002 and 2006, respectively.

He is a coauthor of about 30 papers and of one book. His research interests include the structural and optical properties of nanostructured materials and active photonics devices.

Dr. Navarro-Urrois received Extraordinary Awards from the Experimental and Technical Sciences Division, University of La Laguna.

Alessandro Pitanti was born in Carrara (MS), Italy, in 1981. He graduated in physics and received the M.S. degree from the University of Pisa, Italy, in 2004 and 2006, respectively. He is currently pursuing the Ph.D. degree at the Nanoscience Laboratory, Department of Physics, University of Trento, Italy.

His thesis was on electronic states of Group IV semiconductor quantum wells and multilattices. His current research interests include Si-based resonators and waveguides and sensitization of rare-earth ions for efficient light amplification.

Rita Spano was born in Napoli, Italy, in 1975. She received the M.S. degree in physics from Università di Napoli Federico II, Italy, and the Ph.D. degree from the Nanoscience Laboratory, Department of Physics, University of Trento, Italy, in 2008.

Her research interest is nonlinear optical properties of silicon nanocrystals.

Lorenzo Pavesi was born on November 21, 1961. He received the Ph.D. degree in physics from the Ecole Polytechnique Federale of Lausanne, Switzerland, in 1990.

He is a Professor of experimental physics with the University of Trento, Italy, where he became an Assistant Professor in 1990, an Associate Professor in 1999, and full Professor in 2002. He leads the Nanoscience Laboratory and is Dean of the Ph.D. School in Physics. He is the Director of the professional master in nano- and microsystems. His research activity concerns the optical properties of semiconductors. Recently, he has concentrated on Si-based photonics. His interests encompass also optical sensors or biosensors and solar cells. In silicon photonics, he is one of the worldwide recognized experts. He has organized several international conferences, workshops, and schools and is a frequently invited speaker. He is an author or coauthor of more than 250 papers, author of several reviews, editor of more than ten books, and author of two books. He has received six patents. He is in the Editorial Board of *Research Letters in Physics* and was on the Editorial Board of *Journal of Nanoscience and Nanotechnologies*, the Directive Council of LENS (Florence), and the Board of Delegates of E-MRS. He holds an H-number of 35.